Proteomic Characterization of Ubiquitin Carboxyl-Terminal Hydrolase 19 Deficient Cells Reveals a Role for USP19 in the Secretion of Lysosomal Proteins

Authors

Simone Bonelli, Margot Lo Pinto, Yihong Ye, Stephan A. Müller, Stefan F. Lichtenthaler, and Simone Dario Scilabra

Correspondence

sdscilabra@fondazionerimed.com

Graphical Abstract

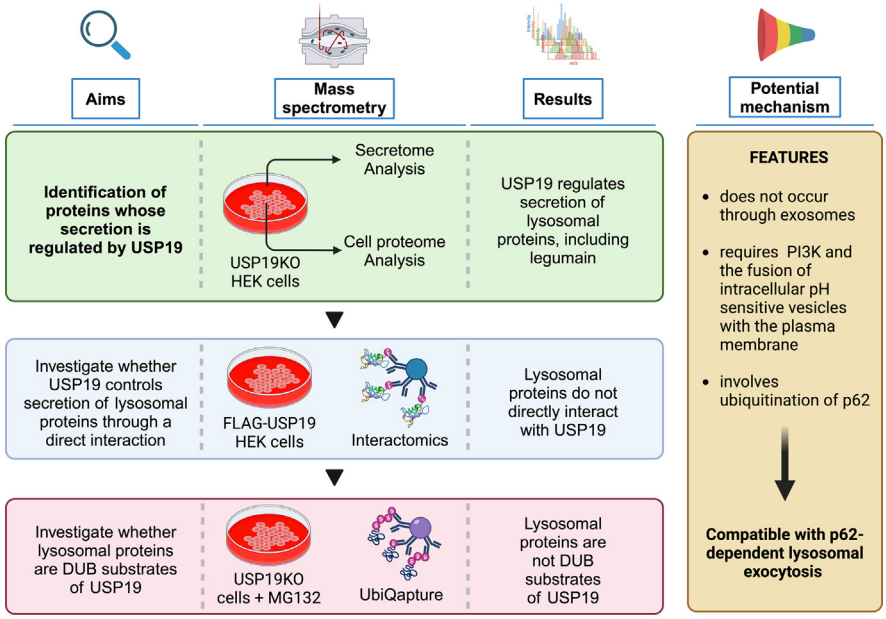

In Brief

USP19 is a unique ER-anchored deubiquitinase that stabilizes proteins and prevents their ER-associated degradation. USP19 also facilitates the unconventional secretion of aggregation-prone proteins like α-synuclein and tau through the misfolded-associated protein secretion (MAPS) pathway. Using high-resolution proteomics, we found that USP19 regulates the secretion of lysosomal proteins, such as legumain (LGMN), via a mechanism resembling p62-dependent lysosomal exocytosis. This study links USP19 to lysosomal protein secretion and sheds light on its broader regulatory roles.

Highlights

- USP19 is a deubiquitinase involved in the unconventional secretion of misfolded proteins.
- High-Resolution Proteomics Uncovers USP19 Role in Lysosomal Protein Secretion.
- USP19 regulates lysosomal protein secretion through a mechanism resembling p62-dependent lysosomal exocytosis.

2024, Mol Cell Proteomics *23*(*11*), 100854

https://doi.org/10.1016/j.mcpro.2024.100854

Proteomic Characterization of Ubiquitin Carboxyl-Terminal Hydrolase 19 Deficient Cells Reveals a Role for USP19 in the Secretion of Lysosomal Proteins

Simone Bonelli[1,2], Margot Lo Pinto[1], Yihong Ye[3], Stephan A. Müller[4,5], Stefan F. Lichtenthaler[4,5,6], and Simone Dario Scilabra[1,*]

Ubiquitin carboxyl-terminal hydrolase 19 (USP19) is a unique deubiquitinase, characterized by multiple variants generated by alternative splicing. Several variants bear a C-terminal transmembrane domain that anchors them to the endoplasmic reticulum. Other than regulating protein stability by preventing proteasome degradation, USP19 has been reported to rescue substrates from endoplasmic reticulum–associated protein degradation in a catalytic-independent manner, promote autophagy, and address proteins to lysosomal degradation *via* endosomal microautophagy. USP19 has recently emerged as the protein responsible for the unconventional secretion of misfolded proteins including Parkinson's disease–associated protein α-synuclein. Despite mounting evidence that USP19 plays crucial roles in several biological processes, the underlying mechanisms are unclear due to lack of information on the physiological substrates of USP19. Herein, we used high-resolution quantitative proteomics to analyze changes in the secretome and cell proteome induced by the loss of USP19 to identify proteins whose secretion or turnover is regulated by USP19. We found that ablation of USP19 induced significant proteomic alterations both in and out of the cell. Loss of USP19 impaired the release of several lysosomal proteins, including legumain (LGMN) and several cathepsins. In order to understand the underlaying mechanism, we dissected the USP19-regulated secretion of LGMN in several cell types. We found that LGMN was not a deubiquitinase substrate of USP19 and that its USP19-dependent release did not require their direct interaction. LGMN secretion occurred by a mechanism that involved the Golgi apparatus, autophagosome formation, and lysosome function. This mechanism resembled the recently described "lysosomal exocytosis," by which lysosomal hydrolases are secreted, when ubiquitination of p62 is increased in cells lacking deubiquitinases such as USP15 and USP17. In conclusion, our proteomic characterization of USP19 has identified a collection of proteins in the secretome and within the cell that are regulated by USP19, which link USP19 to the secretion of lysosomal proteins, including LGMN.

The ubiquitin-proteasome system (UPS) is a major proteolytic system that controls protein stability and therefore plays crucial roles in many biological processes, including DNA repair, stress responses, and cell proliferation (1, 2). Ubiquitination, the biochemical reaction by which proteins are conjugated with ubiquitin and targeted to proteasome for degradation, is reversible by the action of deubiquitylating enzymes (DUBs), which remove ubiquitin conjugates from ubiquitinated substrates. The DUB family comprises about 100 members in mammals, among them the ubiquitin carboxyl-terminal hydrolase 19 (USP19) possesses some unique features.

While other DUBs are soluble in the cytoplasm, USP19 is anchored to the endoplasmic reticulum (ER) through a transmembrane C-terminal domain (3). Through its DUB activity, USP19 controls the stability of a number of proteins, preventing them from proteasomal degradation. For instance, USP19 inhibits the degradation of TGF-beta activated kinase 1, thereby modulating the NF-kB signaling pathway and immune responses (4). In addition, it mediates the deubiquitination of the retinoic acid-receptor–related orphan nuclear receptor γ (RORγt), a master regulator of T helper 17 during cell differentiation (5). As a consequence, USP19 may be involved in the pathogenesis of autoimmune diseases that involve T helper 17 cells such as Crohn's and multiple

From the [1]Proteomics Group of Ri.MED Foundation, Research Department IRCCS ISMETT (Istituto Mediterraneo per i Trapianti e Terapie ad Alta Specializzazione), Palermo, Italy; [2]Department of Biological, Chemical and Pharmaceutical Sciences and Technologies (STEBICEF), University of Palermo, Palermo, Italy; [3]Laboratory of Molecular Biology, National Institute of Diabetes, Digestive and Kidney Diseases, National Institutes of Health, Bethesda, Maryland, USA; [4]Neuroproteomics Department, German Center for Neurodegenerative Diseases (DZNE), Munich, Germany; [5]Neuroproteomics, School of Medicine and Health, Klinikum rechts der Isar, Technical University of Munich, Munich, Germany; [6]Munich Cluster for Systems Neurology (SyNergy) Munich, Germany

*For correspondence: Simone Dario Scilabra, sdscilabra@fondazionerimed.com.

https://doi.org/10.1016/j.mcpro.2024.100854

sclerosis. Interestingly, USP19 has emerged as a multifunctional protein, which not only regulates protein stability by proteasomal degradation but also promotes lysosomal degradation of TANK-binding kinase 1, a major activator of type I interferon signaling (6). Furthermore, USP19 regulates autophagy and antiviral immune responses by the stabilization of beclin-1, an initiator of the autophagic process (7). USP19 can also promote protein translocation into late endosomes *via* endosomal microautophagy (8, 9).

USP19 has recently been implicated in the unconventional secretion of misfolding-prone proteins *via* the misfolding-associated protein secretion (MAPS) pathway (9). The ubiquitin-specific protease domain of USP19 possesses a chaperone activity capable of sensing and recruiting misfolded proteins to the surface of the ER. Misfolded proteins are then delivered to a pre-endosomal compartment akin to the previously reported compartment of unconventional protein secretion (CUPS) (10). The secretion of misfolded proteins involves HSC70, a chaperone protein that bridges the binding of USP19 to a CUPS-associated protein, DnaJ homolog subfamily C member 5 (8, 11). The CUPS-derived vesicles may fuse with the plasma membrane, leading to the release of USP19 cargoes to the extracellular space. This has been recently characterized as a novel protein quality control mechanism that supplements proteasome- and lysosome-mediated clearance of misfolded proteins, preventing the accumulation and aggregation of misfolded proteins. A number of proteins linked to neurodegenerative diseases including α-synuclein (implicated in Parkinson's disease), tau (a microtubule binding protein implicated in Alzheimer's disease), poly-glutamine–containing ataxin 3 (SCA3, involved in can spinocerebellar ataxia 3), SOD1 and TDP43 (associated to amyotrophic lateral sclerosis) have been already reported to undergo USP19-mediated MAPS (11, 12).

Herein, we used an innovative workflow for secretome analysis to identify additional proteins whose secretion could be regulated by USP19. As expected from such a multifunctional protein, we found that ablation of USP19 promotes major changes in the cell secretome. Loss of USP19 impairs release of lysosomal proteins, including legumain (LGMN) and a number of cathepsins. We found that the USP19-dependent secretion of LGMN occurred by a brefeldin A and 3-methyladenine–sensitive mechanism that involves the Golgi apparatus and autophagosome formation, and it is increased by chloroquine that impairs lysosomal function. This resembles a recently discovered mechanism of "lysosomal" exocytosis that is dependent on p62 ubiquitination and that is regulated by DUBs.

EXPERIMENTAL PROCEDURES

Experimental Design and Statistical Rationale

- Analysis of USP19KO secretome and cell proteome. To analyze changes in the secretome and cell proteome of USP19KO cells compared to WT, conditioned media and cell lysates were collected from six biological samples of USP19KO human embryonic kidney 293T (HEK)s and six of WT HEKs. This results in 24 samples, 12 conditioned media and 12 lysates. Data-dependent acquisition was used for label-free quantification of protein intensities in each sample. The software MaxQuant was used for label-free quantification with the normalization option enabled. Two thousand three hundred thirty six proteins were identified in the secretome of USP19KO and WT cells, which were filtered based on valid values found for at least three out of twelve total samples. This reduced the matrix to 1676 proteins that were analyzed with Perseus for the statistical analysis of their change in USP19KO and WT cells. Five thousand eight hundred proteins were identified in the lysates of USP19KO and WT cells, which were reduced to 4667 based on three valid values out of twelve total samples. Student *t* test and false discovery rate (FDR) correction were used to analyze the statistical significance of changes in protein intensity between USP19KO and WT HEKs. Sample preparation, LC-MS/MS analysis, proteomic data analysis, and statistical evaluation of changes are detailed in the "High-resolution analysis of USP19KO cell secretome and proteome" section below. Raw data have been uploaded to ProteomeXchange through the PRIDE repository with the accession code PXD055064 and 10.6019/PXD055064.
- Analysis of interactors of USP19. Four biological replicates of USP19-FLAG expressing HEKs and four biological replicates of MXRA8-FLAG expressing HEKs were used for immunoprecipitation with an anti-FLAG resin. Eight immunoprecipitated samples were analyzed by label-free quantification (LFQ) – data-independent acquisition (DIA) with the DIA-NN software. Five thousand three hundred five proteins were identified, which were reduced to 5208 by filtering based on three valid values out of four found in at least one group of samples (either USP19 or control) and further analyzed by Student *t* test and FDR correction to assess the statistical significance of changes in protein intensity between USP19KO and WT HEKs with Perseus software. Raw data have been uploaded to ProteomeXchange through the PRIDE repository with the accession code PXD055081.
- Analysis of DUB substrates of USP19. To analyze changes in the level of ubiquitinated proteins from the extracts of USP19KO and WT HEKs, ubiquitinated proteins were isolated from three biological replicates of USP19KO HEKs and from three biological replicates of WT HEKs and from three biological replicates of MG132-treated USP19KO cells and three biological replicates of MG132-treated WT HEKs. This results in 12 samples, each of which was loaded onto an acrylamide gel and proteins separated by SDS-PAGE electrophoresis. Eleven slices were excited from each lane, and proteins subjected to in-gel digestion. After extracting peptides from each slice, peptides from each sample were pulled together for further analysis. Thus, 12 samples were analyzed by LFQ – DIA with the DIA-NN software. Six hundred sixty nine total proteins were identified in USP19KO and WT cells, which were reduced to 460 based on three valid values found in at least one group. These proteins were further analyzed by the Student's *t* test and FDR correction to assess the statistical significance of changes in protein intensity between USP19KO and WT HEKs. Raw data have been uploaded to ProteomeXchange through the PRIDE repository with the accession code PXD055118.

High-Resolution Analysis of USP19KO Cell Secretome and Proteome

Cell Cultures—USP19KO and control WT human embryonic kidney 293T (USP19KO and WT HEK) cells were generated by CRISPR-Cas9, as reported by Lee *et al*. (9) USP19WT and KO cells were maintained in high glucose DMEM with 10% FBS, 100 U/ml penicillin, and 100 U/ml streptomycin at 37 °C in 5% CO_2.

Sample Processing and Mass Spectrometry Analysis—USP19KO and WT HEK cells were grown in 10 cm dishes until confluence, then washed twice, and incubated in serum-free DMEM for 48 h. ApoTox-Glo Triplex Assay (from Promega) was used to assess viability, cytotoxicity, and apoptosis of USP19KO and WT HEKs, according to the manufacturer's instructions. Ten milliliters of conditioned media were harvested, centrifuged (2000*g* for 10 min) to remove cell debris, and concentrated by Vivaspin protein concentrator spin columns with a 10 kDa molecular weight cut-off (from Sartorius). Protein concentration was measured by using a colorimetric 660 nm microBCA assay (Thermo Fisher Scientific). In addition, cells were lysed with SDT buffer [4% w/v SDS; 100 mM Tris HCl pH 7.6; 0.1 M DTT] and proteins quantified by a colorimetric 660 nm microBCA assay. A protein amount of 30 μg per sample, either from conditioned media or lysates, was subjected to proteolytic digestion using the filter-assisted sample preparation protocol with 10 kDa Vivacon spin filters (Sartorius) (13). Generated peptides were desalted by stop-and-go extraction (STAGE) on reverse phase C18 (14) and eluted in 40 μl of 60% acetonitrile in 0.1% formic acid. The volume was reduced in a SpeedVac (Thermo Fisher Scientific) and the peptides were resuspended in 10 μl of 0.1% formic acid, prior to being analyzed by LC-MS/MS setup comprising a nanoLC system (EASY-nLC 1000, Proxeon – part of Thermo Fisher Scientific) with an in-house packed C18 column (30 cm × 75 μm ID, ReproSil-Pur 120 C18-AQ, 1.9 μm, Dr Maisch GmbH) coupled online *via* a nanospray flex ion source equipped with a PRSO-V1 column oven (Sonation) to a Q-Exactive mass spectrometer (Thermo Fisher Scientific). One microgram of peptides were separated using a 180 min binary gradient of water and acetonitrile containing 0.1% formic acid at 50 °C column temperature. The mass spectrometer was operated in positive mode and a full MS1 scan was acquired at a resolution of 70,000 with a scan range of 300 to 1400 m/z. Automatic gain control (AGC) target was set to 3×10^6 with a maximum injection time of 50 ms. dd-MS2 scan on the TopN 10 most intense peptide ions per full MS1 scan for peptide fragmentation was performed at a resolution of 17,500 with an isolation width of 2 m/z and covering a scan range of 200 to 2000 m/z. AGC target was set to 1×10^5 with a maximum injection time of 75 ms and a normalized collision energy of 25%. Dynamic exclusion was set to 120 ms.

Proteomic Data Analysis—The data were analyzed by the software MaxQuant (maxquant.org, Max-Planck Institute Munich - version 2.6.1.0), by using standard parameters (15). The MS data were searched against a reviewed canonical fasta database of *Homo sapiens* from UniProt (download: May 29, 2024; 20,590 entries). Trypsin/P was defined as protease and a maximum of two missed cleavages were allowed for database search. The option first search was used to recalibrate the peptide masses within a window of 20 ppm. The main search peptide tolerance was set to 4.5 ppm and the peptide fragment mass tolerance to 20 ppm. Carbamidomethylation of cysteines was set as a static modification, while protein N-terminal acetylation and methionine oxidation were set as variable modifications. Label-free quantification (LFQ) was used to quantify protein intensities required at least two ratio counts of unique peptides. Unique and razor peptides were used for quantification. A FDR less than 1% was set for peptides and proteins. Match between runs was enabled with a match time window of 2 min for the transfer of identification. The Perseus software (copyright of Max Planck Institute of Biochemistry) was used to analyze the statistical significance of changes in protein levels between USP19KO and WT HEK cells. LFQ values were Log2 transformed and a two-sided Student's *t* test was used for statistical analysis. An FDR to 0.05 and a minimal fold change (s0) to 0.1 were set as the threshold for statistically significant alterations. An FDR to 0.01 was set to identify a subgroup of most altered proteins.

Subcellular Location and Gene Ontology Analysis

GO and KEGG Analysis—Gene ontology (GO) and Kyoto Encyclopedia of Genes and Genomes (KEGG) analysis was performed by using Enrichr, an enrichment analysis web-based tool developed in the Ma'ayan Lab at the Icahn School of Medicine (16). The R studio software (17) was used to display GO and KEGG results in a dotplot.

Subcellular Location Analysis—Subcellular location of proteins detected by proteomics was analyzed according to UniProt annotations (July 20, 2024). In order to evaluate the enrichment of proteins with a specific subcellular location within those that were altered in the secretome of USP19KO cells, it was compared in a logarithmic scale the ratio between regulated proteins with a specific subcellular location (Reg SL) and the total number of regulated proteins (Reg tot), to the ratio between the total number of proteins with a certain subcellular location (TOT SL) and the total number of proteins detected by the analysis (TOT). Thus, the following formula was applied

$$Log\,2\frac{\left(\frac{Reg\ SL}{Reg\ tot}\right)}{\left(\frac{TOT\ SL}{TOT}\right)}\ \text{e.g. for lysosomal proteins}$$

$$Log\,2\frac{\left(\frac{Reg\ Lysosome}{Reg\ tot}\right)}{\left(\frac{TOT\ lysosome}{TOT}\right)}=Log\,2\frac{\left(\frac{25}{238}\right)}{\left(\frac{64}{1676}\right)}=1.462$$

In order to evaluate whether proteins with certain subcellular locations were enriched or diminished among altered proteins in USP19KO cells, the ratio between upregulated proteins (Up SL) and downregulated proteins (Down SL) with a certain location was compared to the ratio between the total number of upregulated (Up TOT) and downregulated proteins (Down TOT). The following formula was applied:

$$Log\,2\frac{\left(\frac{Up\ SL}{Down\ SL}\right)}{\left(\frac{Up\ TOT}{Down\ TOT}\right)}\ \text{e.g. for lysosomal proteins}$$

$$Log\,2\frac{\left(\frac{Up\ Lysosome}{Down\ lysosome}\right)}{\left(\frac{Up\ TOT}{Down\ TOT}\right)}=Log\,2\frac{\left(\frac{1}{24}\right)}{\left(\frac{14}{49}\right)}=-2.777$$

Characterization of Extracellular Vesicles Released by USP19KO Cells

For each experiment, USP19KO and WT were grown in vesicles-deprived complete medium in three 175 cm^2 flasks until confluence, washed twice in PBS, and incubated in serum-free medium for 48 h. Thirty milliliters of conditioned media were collected and further processed for exosome isolation as described by Théry *et al*. (18). In brief, conditioned media were sequentially centrifuged at 300*g* for 5 min and 2000*g* for 10 min, to get rid of cells and debris. Then, supernatants were centrifuged at 100,000*g* for 30 min and subsequently at 120,000*g* for 70 min. Pelleted extracellular vesicles were collected with 100 ml PBS and characterized (number of vesicles per cells; diameter) by a NanoSight NS3000 (Malvern Panalytical, part of

Spectris plc). The NanoSight instruments utilize Nanoparticle Tracking Analysis to characterize nanoparticles from 10 nm - 1000 nm by using both light scattering and Brownian motion in order to obtain the nanoparticle size distribution.

Validation of Potentially Regulated Proteins by Western Blotting

USP19KO or WT HEK cells were seeded in poly-D-Lysine–coated 6-well plates ($1{\cdot}10^6$ cells/well) and grown for 24 h in complete media. Then, cells were washed twice with PBS and incubated 48 h in serum-free media. Conditioned media were concentrated by precipitation with 5% trichloroacetic acid (Sigma Aldrich), resuspended in Laemmli buffer, and loaded onto an acrylamide gel for electrophoresis. After electrophoretic separation, proteins were blotted to a PVDF membrane using the Trans-Blot Turbo transfer system (BioRad) and detected by specific antibodies. Cells were washed with ice-cold PBS and lysed on ice with STET buffer (100 mM sodium chloride, 10 mM Tris–HCl pH 8.0, 1 mM EDTA, and 5% Triton X-100) containing protease inhibitors (Sigma). Protein concentration in each sample was measured by BCA assay, and 20 μg of protein was loaded onto an acrylamide gel, transferred onto a PVDF membrane, and detected by specific antibodies. Bands corresponding to each protein were quantified by using Image Lab software (Bio-Rad). Bands corresponding to USP19KO samples were normalized to the mean of the original non-normalized control values (USP19WT cells). A two-sided Student's *t* test was used to evaluate proteins statistically significantly regulated, with a *p*-value less than 0.05 that was set as the significance threshold.

Two different constructs were used to rescue USP19 expression in USP19KO HEK cells, pRK-FLAG-USP19 (plasmid # 78597 from Addgene), and pEGFP-rUSP19ER (plasmid # 155247, Addgene), while pCMV3-C-GFPSpark (SinoBiological Eschborn) was used as a control. To knock-down USP19, HTB94, LX-2, HeLa, or U251 cell lines were grown to 70% confluence in a 6-well plate. Cells were transfected with Lipofectamine RNAiMAX reagent (Invitrogen, part of Thermo Fisher Scientific) and 40 pmol USP19 siRNA-1 (5′-GGCGUGACAAGAUCAAUGA-3′) or control siRNA purchased from Invitrogen as reported by Lee *et al* (9). USP19WT HEK cells were grown in poly-D-Lysine–coated 6-well plates. Then, they were incubated in serum-free media containing either 0.35 μM brefeldin A (Sigma B7651), 0.5 μM MG132 (Sigma C2211), 10 nM chloroquine (Sigma C6628), 10 mM 3-methyladenine (3-MA, Sigma M9281), 10 μM GW4869 (Sigma), 80 μM Dynasore (Sigma 324410), or DMSO (WAK-Chemie Medical GmbH) for 24 h. Conditioned media and cell lysates were harvested and processed as described above. Proteins were loaded onto a gel and immunoblotted with specific antibodies. Bands corresponding to each protein were quantified and normalized to the mean of the original non-normalized control values, and a two-sided Student's *t* test was used to evaluate the statistical significance of protein changes. Antibodies used in this study are listed in Table 1 below.

Analysis of the USP19 Interactome

HEK cells were grown in 10 cm poly-D-Lysine–coated dishes until 70% confluent and transfected with 15 μg of pRK-FLAG-USP19 (Addgene, plasmid #78597), pcDNA3.1-FLAG-MXRA8, or empty vector using 30 μl of Lipofectamine 3000 (Invitrogen) in Opti-MEM I (Gibco). After 16 h, cells were washed and incubated in serum-free DMEM for further 48 h. Then, cells were washed with ice-cold PBS and lysed on ice with 1 ml of lysis buffer (50 mM Tris–HCl pH 7.4150 mM sodium chloride, 1 mM EDTA, and 1% Triton X-100) containing protease inhibitors (Sigma). Cell lysates were cleared by centrifugation (14,000*g*; 4 °C; 15 min) and supernatants were applied to an anti-FLAG M2 Affinity Gel (Sigma-Aldrich) for immunoprecipitation. Bound proteins were eluted by incubating the beads with 120 μl of TBS containing 150 ng/μl 3X FLAG peptide (Sigma-Aldrich) for 1 h at 4 °C. Thirty microliters of eluted proteins were used to evaluate co-immunoprecipitation of LGMN with USP19 by immunoblotting and 90 μl of proteins further processed for the proteomic analysis.

Eluted proteins were subjected to tryptic digestion with filter-assisted sample preparation using filter columns with a 10 kDa cut-off, as described above. This method allowed the removal of FLAG peptide, whose molecular weight is below 3 kDa, before the tryptic digestion of eluted proteins. After desalting through STAGE-tips, 1 μg of generated peptides were applied to LC-MS/MS analysis using a nanoLC system (Vanquish Neo UHPLC — Thermo Fisher Scientific) coupled online to an Exploris 480 mass spectrometer (Thermo Fisher Scientific). Peptides were separated on Acclaim PEPMap C18 column (25 cm × 75 μm ID, Thermo Fisher Scientific) with 250 nl/min flow using a binary gradient of water and acetonitrile supplemented with 0.1% formic acid for 130 min. DIA was used for LFQ. DIA was performed using an MS1 full scan followed by 60 sequential DIA windows with an overlap of 1 m/z and window placement optimization option enabled. Full scans were acquired with a resolution of 120,000 with a scan range of 400 to 1000 m/z, AGC of 3×10^6, and maximum injection time of 50 ms. Afterwards, 60 isolation windows were scanned with a resolution of 30,000, an AGC of 8×10^5, and maximum injection time was set as auto to achieve the optimal cycle time. Collision-induced dissociation fragmentation was induced with 30% of the

TABLE 1
List of antibodies used in this study

Antibody	Clone	Host	Code	Company	Dilution
Calnexin		Rabbit	ADI-SPA-860-F	Enzo Life Science	1:1000
Clusterin	B-5	Mouse	Sc-5982	Santa Cruz	1:2000
CTSB	173,317	Rat	mab965	R&D	1:1000
CTSD		Rabbit	nbp1-50682	Novus Biological	1:1000
FLAG M2	F3165	Mouse	F1804	Sigma-Aldrich	1:1000
HSP90 α/β	F8	Rabbit	SC13119	Santa Cruz	1:2000
Legumain		Goat	AF2199	R&D	1:1000
LAMP1		Rabbit	ab24170	Abcam	1:1000
LC3B		Rabbit	NB100-2220	Novus Biological	1:1000
p62	D1Q5S	Rabbit	#39749	Cell Signalling	1:1000
SNCA		Rabbit	GTX112799	GeneText	1:1000
Ubiquitin	P4G7	Mouse	838701	BioLegend	1:1000
USP19		Rabbit	A301-587A	Bethyl Laboratories	1:1000
β-actin	C-4	Mouse	sc-47778	Santa Cruz	1:1000

normalized higher-energy collisional dissociation. The data were analyzed using the software DIA-NN (version 1.8.1) and a predicted library generated from in silico digestion of a reviewed canonical fasta database of *H. sapiens* from UniProt (download: May 29, 2024; 20,590 entries), with cleavages at K* and R*, two missed cleavages allowed, and N-terminal methionine excision enabled. Peptide length range was set at 6 to 30 residues; precursor charge range at 2 to 5; precursor m/z at 400 to 1000 and fragment ion m/z range at 200 to 1800. Cysteine carbamidomethylation was enabled as a fixed modification, methionine oxidation and N-terminal acetylation as variable modification, and maximum number of variable modifications was set to 1. Match between runs option was enabled and Mass accuracy, MS1 accuracy, and Scan window was set to 0. Protein inference was set to gene and Neural network classifier to single-pass mode. Quantification strategy was set to Robust LC (high precision) and cross-run normalization to RT-dependent. Smart profiling was used for library generation and Speed and RAM usage set to optimal results. The FDR for precursors identification was set at 1%. The Perseus software was used to analyze the statistical significance of changes in the abundance of proteins co-eluted with USP19-FLAG and MXRA8-FLAG. LFQ intensities were Log2 transformed and a two-sided Student's *t* test was used for statistical analysis, with an FDRFDR set to 0.05 and a minimal fold change (s0) to 0.1.

Identification of DUB Substrates of USP19

Analysis of Ubiquitinated Legumain in USP19KO HEK Cells—USP19KO and WT HEK cells were grown on poly-D-Lysine–coated 6-well plates until 70% confluent, then washed twice with PBS, and incubated for 48 h in serum-free media with or without 0.5 μM MG132 (Sigma) or DMSO. Then, cells were washed twice with ice-cold PBS and lysed on ice with 200 μl Pierce RIPA buffer (Thermo Fischer Scientific) supplemented with protease inhibitors (Sigma) and 15 μM MG132 (Sigma). Lysates were clarified at 14,000 rpm at 4 °C for 15 min and total protein concentration was measured by BCA assay. Two hundred fifty micrograms of proteins were diluted with 1 ml of PBS buffer and applied to the UBI-QAPTURE-Q kit (Enzo Life Sciences) for the enrichment of ubiquitinated proteins, according to the manufacturer's instructions. Proteins were eluted with 100 μl of 2 × Laemmli sample buffer (Bio-Rad) by boiling at 95 °C for 5 min. Fifteen microliters of eluted proteins were loaded onto an acrylamide gel for SDS-PAGE electrophoresis and immunoblotting for LGMN.

Unbiased Identification of Differentially Ubiquitinated Proteins in USP19KO Cells—To perform unbiased proteomic analysis of ubiquitinated proteins in USP19KO and WT cells, 40 μl of proteins eluted from the UBI-QAPTURE-Q kit were separated by SDS-PAGE electrophoresis, cut into 11 horizontal slices at equal height, and subjected to tryptic in-gel digestion (19). Briefly, proteins were fixed and stained using the Novex Colloidal Blue Staining Kit (Invitrogen). Each gel lane was cut in 1.5 × 5 mm slices with a gel-cutter, and each slice destained with 200 mM ABC in 50% acetonitrile for 15 min at 37 °C. Proteins were reduced with 50 mM DTT in 25 mM ABC for 30 min at 37 °C and alkylated by incubation with 25 mM ABC buffer containing 40 mM iodoacetamide for 15 min at 37 °C. Then, gel slices were digested at 37 °C overnight using 300 ng trypsin per fraction. Peptides were extracted with 40% acetonitrile supplemented with 0.1% formic acid, dried by vacuum centrifugation, and reconstituted in 0.1% formic acid. Then, peptides from different slices of each lane were pulled together and desalted by STAGE-Tips (14).One microgram of peptides were subjected to LC-MS/MS analysis using the set comprising a Vanquish Neo UHPLC coupled online to an Exploris 480 mass spectrometer, as described above. The data were analyzed using the software DIA-NN (version 1.9) and a predicted library generated from in silico digestion of a reviewed canonical fasta database of *H. sapiens* from UniProt (download: May 29, 2024; 20,590 entries), with cleavages at K* and R*, two missed cleavages allowed, and N-terminal methionine excision enabled. Peptide length range was set at 6 to 30 residues; precursor charge range at 2 to 5; precursor m/z at 400 to 1000 and fragment ion m/z range at 200 to 1800. Cysteine carbamidomethylation was enabled as a fixed modification, methionine oxidation and N-terminal acetylation enabled as variable modification, and maximum number of variable modifications set to 1. Peptidoforms, Match between runs, and No shared spectra options were enabled and Mass accuracy, MS1 accuracy, and Scan window set to 0. Protein inference was set to gene and neural network classifier to single-pass mode. Quantification strategy was set to QuantUMS (high precision) and cross-run normalization to RT-dependent. IDs, RT, & IM profiling was used for library generation and Speed and RAM usage set to optimal results. The FDR for precursors identification was set at 1%. LFQ intensities were Log2 transformed and significant changes in the intensity of ubiquitinated proteins extracted from USP19KO and WT cells were assessed by a Student's *t* test, with an FDR set to 0.05 and a minimal fold change (s0) to 0.1.

Measurement of LAMP1 at the Cell Surface by Flow Cytometry

USP19KO and WT HEK cells were grown in 10 cm dishes until confluent, then washed twice, and incubated in serum-free DMEM for 48 h and finally harvested with TrypLE reagent (Gibco, part of Thermo Fisher Scientific). 1.6×10^6 USP19KO and WT HEK cells were stained with 10 μl of BD Pharmingen FITC Mouse Anti-Human CD107a (LAMP1) (clone H4A3 from BD Bioscience) or isotype BD Pharmingen FITC Mouse Anti-Human IgG [G18-145] (BD Bioscience) at room temperature for 30 min according to the manufacturer's instruction. Then, cells were washed with PBS and resuspended in 400 μl of PBS. Five microliters of 7-AAD viability staining solution was added to the mixture to assess cell viability. Then, cells were analysed with a FACS Celesta SORP flow cytometer and FACS Diva software version 9.0 (BD Biosciences).

RESULTS

Quantitative Proteomics Identifies Proteins Whose Secretion is Regulated by USP19

USP19 has recently been implicated in the secretion of misfolded cytosolic proteins in an unconventional manner when substrates are overexpressed in mammalian cells (9). To identify endogenous proteins whose secretion is regulated by USP19, including proteins that can be unconventionally secreted, we used a method of secretome analysis that allows the detection of cytosolic leaderless proteins in the conditioned media, in addition to secreted and shed transmembrane proteins (20). Indeed, the resolution of this method, which comprises LC-MS/MS analysis and label-free quantification, is high enough to detect low abundant proteins in the conditioned media, such as those proteins that are secreted in an unconventional manner. USP19WT and KO human embryonic kidney 293T (HEK) cells were cultured in serum-free media for 48 h (no evident differences in morphology, viability, cytotoxicity, and apoptosis were found between USP19KO and WT cells at this time – Supplemental Fig. S1). Then, conditioned media were collected and analyzed by LC-MS/MS, followed by LFQ. One thousand six hundred seventy six proteins were identified from the conditioned media of USP19KO and WT cells (Fig. 1, *A* and *B* and Supplemental

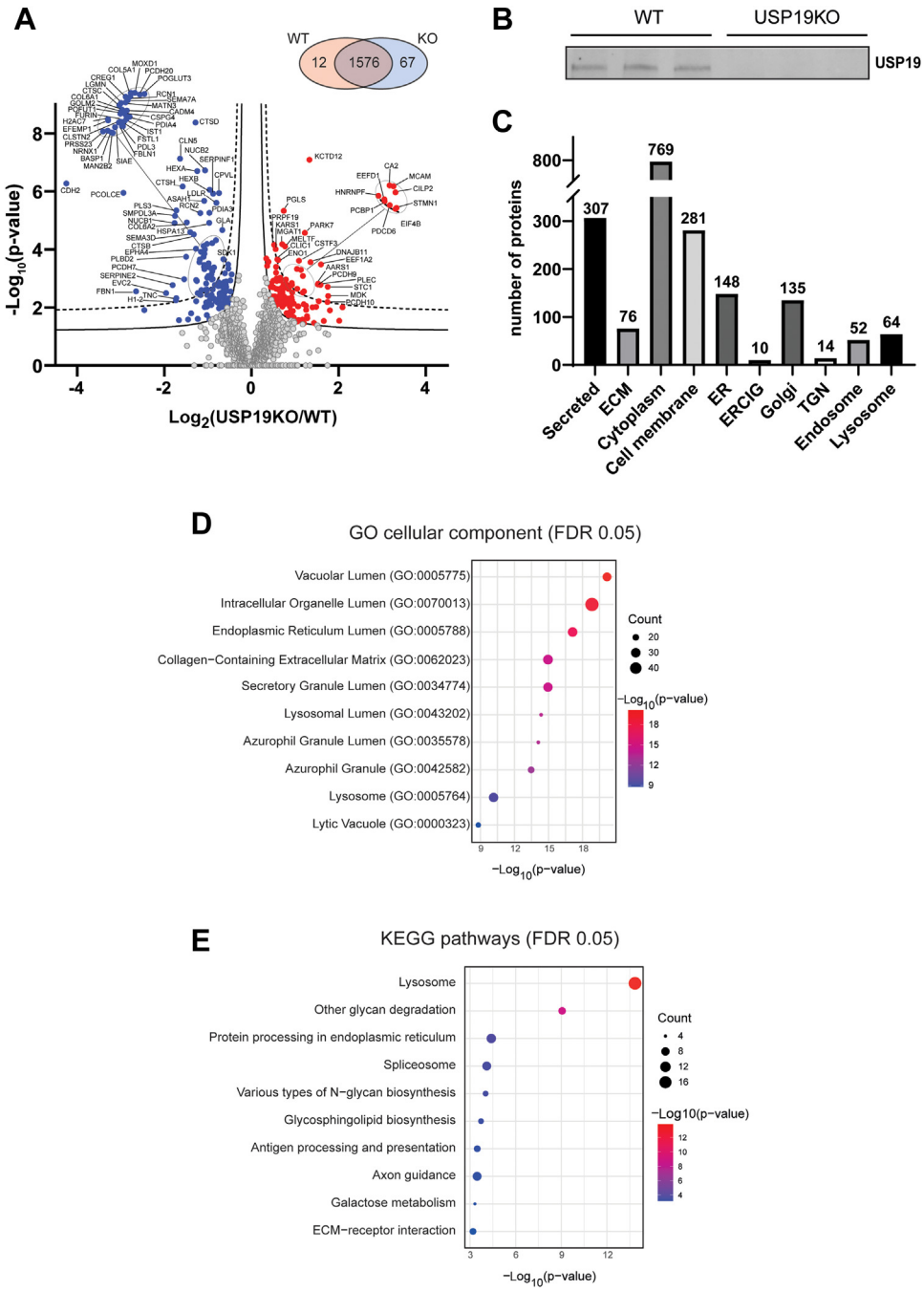

FIG. 1. **A high-resolution mass spectrometry–based approach identifies proteins differentially abundant in the secretome of USP19KO HEK cells.** *A*, volcano plot showing the –Log10 of *p*-values *versus* the Log2 of protein ratio between USP19KO HEK (USP19KO) and USP19WT HEK cells of 1676 proteins (n = 6). Proteins significantly more abundant in the secretome of USP19KO cells are displayed as *red* filled dots, while less abundant proteins are displayed as *blue* filled dots. The *solid black* hyperbolic curves display the FDR at 0.05 and the dashed curves at 0.01. Unaltered proteins are displayed as the *gray* dots below the FDR curve. The Venn diagram in the inset displays the number of proteins identified in the secretome of WT or USP19KO cells and the number of proteins found in both secretomes. *B*, Western blot showing levels of USP19 in WT and USP19KO HEKs (Please note that this blot was made using the anti-USP19 clone A301-586A from Bethyl Laboratories, which was eventually discontinued; all other USP19 blots shown in this study were obtained with the anti-USP19 clone A301-587A from the same vendor). *C*, number and subcellular location of proteins detected in the secretome of USP19KO cells. *D*, gene ontology and (*E*) KEGG pathways analysis of proteins regulated (FDR $p = 0.05$) in USP19KO cells to identify biological functions of USP19.

Table S1). Among them, 307 were proteins annotated as secreted proteins (these are either conventionally secreted or leaderless proteins that are commonly located in the extracellular space, according to UniProt annotation) and 281 as cell membrane, most likely present in the secretome as a consequence of ectodomain shedding. In addition, based on UniProt annotation, the mass spectrometry analysis identified 769 cytoplasmic proteins, many of which were associated with different organelles such as ER (148 proteins), ERGIC (10) Golgi (135, of which 14 associated with the trans-Golgi network), endosome (52), and lysosome (65) (Fig. 1*C* and Table 2, Supplemental Table S1). LFQ analysis displayed that ablation of USP19 affected the level of many proteins in the secretome, with 239 proteins being significantly altered (proteins above the FDR curves, shown as solid black hyperbolic curves in Figure 1*A*; FDR $p = 0.05$; s0 = 0.1), accounting for about 15% of the total proteins detected in conditioned media. Among them, 122 proteins were significantly reduced in the conditioned media of USP19KO cells (Fig. 1*A*). Within this latter group fall proteins potentially secreted in an USP19-dependent manner. As expected, these proteins mostly carried a signal sequence or a transmembrane segment, which target them to the ER-mediated conventional protein secretion pathway. Among proteins reduced in the secretome of USP19KO cells, 49 proteins were annotated as secreted, including procollagen C-endopeptidase enhancer 1 (PCOLCE), fibulin-1 (FBLN1), and a number of cathepsins (CTSB, CTSD and CTSC), and 25 were annotated as cell membrane proteins, including cadherin 2 (CDH2), protocadherin-20 (PCDH20), and amyloid precursor protein (APP). Intriguingly, 55 reduced proteins were not annotated as secreted or cell membrane and therefore potentially secreted by USP19 in an unconventional manner. Belonged to this group are ER- or Golgi-associated proteins, such as nucleobindin-1 and -2, and 24 lysosomal proteins, including LGMN, the α and β subunit of β-hexosaminidase (HEXA and HEXB) and others (Fig. 1*A*, Tables 2 and 3, and Supplemental Table S1). Finally, 20 proteins annotated as cytoplasmic were diminished in condition media (*e.g.* PLS3) and therefore potential novel MAPS cargos. This likely represents a small fraction of physiological MAPS cargoes because the experiments were conducted under serum-depleted culture condition, which, while being necessary to eliminate serum contaminants from the secretome and allow mass spectrometry, is known to diminish USP19-mediated unconventional protein secretion (21). On the other hand, 117 proteins were significantly more abundant in the conditioned media of USP19KO cells, including protocadherin-9 (PCDH9), EMILIN2, BTB/POZ domain-containing protein KCTD12 (KCTD12); protein deglycase DJ-1 (PARK7), and carbonic anhydrase 2 (CA2) (Fig. 1*A* and Supplemental Table S1).

Secretion of Lysosomal Proteins is Deregulated in USP19KO Cells

Proteins affected in USP19KO cells were evaluated using the Enrichr web server for GO and KEGG pathway analysis (16, 22). The GO-Cellular Component analysis found that the major group of proteins altered by the loss of USP19 were those associated with the intracellular organelle lumen (GO:0070013), lysosomal lumen (GO:0005775), vacuolar lumen (GO:0005775), and ER lumen (GO:0005788) (Fig. 1*C* and Supplemental Table S1). Furthermore, KEGG analysis suggested that the lysosome pathway is most affected in the conditioned media of USP19KO HEK cells (Fig. 1*D* and Supplemental Table S1). Levels of more than one third of all lysosomal proteins detected in the secretome were altered as a consequence of USP19 depletion (Table 2 and Fig. 2*A*). Moreover, extracellular matrix (ECM)-associated proteins, cell membrane, endosome, and ER-associated proteins were also altered, although at lesser extent than lysosomal proteins (Fig. 2A). A further analysis found that the large majority of regulated lysosomal proteins were decreased in the secretome of USP19KO cells (Fig. 2*B* and Table 2). Similarly, regulated ER- and endosome-associated proteins diminished, while cytoplasmic proteins augmented (Fig. 2*B* and Table 2).

Unconventional secretion comprises pathways involving the release of extracellular vesicles, primarily exosomes (23). By using nanoparticle tracking analysis, we found that loss of USP19 neither affected the number of released extracellular vesicles nor their size, which was about 100 nm in diameter, characteristic of exosomes (Fig. 2*C*). Altogether, these results suggested that loss of USP19 mainly impairs the secretion of lysosomal and other luminal proteins and confirm previous reports that USP19-mediated secretion pathways do not involve exosome release (9).

We next investigated whether USP19 loss could lead to altered lysosomal function and/or autophagy. Immunoblot analysis displayed that bands corresponding to the late endosomal/lysosomal marker LAMP-1 shifted at slightly

TABLE 2
Subcellular location of proteins detected by secretome analysis of USP19KO cells

Proteins	Secreted	ECM	Cytoplasm	Cell membrane	ER	ERCIG	Golgi	TGN	Endosome	Lysosome
Total (1676 proteins)	307	76	769	281	148	10	135	14	52	64
Altered (238 proteins)	63	14	89	45	34	2	21	2	8	25
Increased (117 proteins)	14	3	69	20	11	1	5	0	3	1
Decreased (121 proteins)	49	11	20	25	23	1	16	2	5	24

TABLE 3
Selected proteins significantly decreased in the secretome of USP19KO HEK293T cells

Protein names	Subcellular localization	Protein IDs	Gene names	Unique peptides	*p*-value	Ratio
Procollagen C-endopeptidase enhancer 1	Secreted	Q15113	PCOLCE	31	1.11E-06	0.13
Fibrillin-1	Secreted, ECM	P35555	FBN1	41	2.81E-03	0.16
Nucleobindin-1	Secreted, Cytoplasm, Golgi	Q02818	NUCB1	34	1.24E-05	0.29
Plastin-3	Cytoplasm	P13797	PLS3	33	4.53E-06	0.30
Cathepsin B	Secreted, Cell memb, Lysosome	P07858	CTSB	19	3.01E-05	0.40
EGF-containing fibulin-like extracellular matrix protein 1	Secreted, ECM	Q12805	EFEMP1	18	1.21E-03	0.42
Beta-hexosaminidase subunit alpha	Lysosome	P06865	HEXA	22	1.97E-07	0.42
Dipeptidyl peptidase 1	Lysosome	P53634	CTSC	19	2.78E-04	0.44
Legumain	Lysosome	Q99538	LGMN	19	2.22E-04	0.44
Neurexin-1	Cell memb	Q9ULB1	NRXN1	27	2.51E-03	0.45
Collagen alpha-1 (V) chain	Secreted, ECM	P20908	COL5A1	14	7.55E-05	0.47
Collagen alpha-1 (VI) chain	Secreted, ECM	P12109	COL6A1	45	3.38E-04	0.47
Reticulocalbin-1	ER	Q15293	RCN1	17	9.93E-05	0.48
Nucleobindin-2	Secreted, Cytoplasm, ER, Golgi	P80303	NUCB2	19	1.90E-07	0.48
Epididymis-specific alpha-mannosidase	Secreted	Q9Y2E5	MAN2B2	22	2.41E-03	0.49
Heat shock 70 kDa protein 13	ER	P48723	HSPA13	18	1.22E-05	0.51
Protein disulfide-isomerase A3	ER	P30101	PDIA3	34	5.49E-06	0.51
Follistatin-related protein 1	Secreted	Q12841	FSTL1	25	7.26E-04	0.53
Fibulin-1	Secreted, ECM	P23142	FBLN1	28	1.08E-03	0.53
Protocadherin-20	Cell memb	Q8N6Y1	PCDH20	18	6.09E-05	0.54
Probable serine carboxypeptidase CPVL	Exosomes	Q9H3G5	CPVL	18	1.19E-06	0.54
Protein disulfide-isomerase A4	ER	P13667	PDIA4	35	4.16E-04	0.55
Pigment epithelium-derived factor	Secreted	P36955	SERPINF1	26	1.13E-06	0.60
Alpha-galactosidase A	Lysosome	P06280	GLA	15	2.14E-05	0.63

Protein name: proteins less abundant in the conditioned media of USP19KO HEK cells above the FDR curve (FDR $p = 0.05$; s0 = 0.1) and with a protein score higher than 180; Protein ID: UniProt accession number of the protein. Gene names: UniProt gene name associated with each protein; Unique peptides: Number of unique peptides identified in the LC/MS-MS analysis for each protein; *p*-value: for six biological replicates. Ratio: mean ratio of label-free quantification intensities between USP19WT and KO HEK cells (n = 6).

higher molecular weight, likely as a consequence of higher glycosylation, suggesting that endosomal/lysosomal homeostasis could be disrupted when USP19 was ablated (Fig. 2, *E* and *F*) (24). The ubiquitin-associated protein p62 and the conversion of soluble microtubule-associated protein light chain 3 (LC3-I) to lipid-bound LC3-II are commonly used to monitor autophagic flux (25). We found that levels of p62 reduced as processed LC3B-II levels increased in USP19KO cells, suggesting that loss of USP19 could lead to altered autophagy (Fig. 2, *E* and *F*).

Analysis of the Cell Proteome to Identify Proteins Regulated by USP19

Since USP19 is known to regulate protein stability as well as secretion, depletion of USP19 is expected to re-sculpt the cellular proteome. To identify proteins regulated by a USP19-dependent manner, we analyzed lysates of USP19KO and WT cells by quantitative proteomics. LFQ analysis identified 4667 proteins in the lysate of USP19KO and WT cells (Fig. 3*A*), comprising 120 secreted, 12 ECM, 2032 cytoplasmic, 474 cell membrane, 497 ER, 275 Golgi, 70 TGN, 218 endosome, and 122 lysosome proteins (Fig. 3*B*). In addition, the analysis identified 1750 nuclear proteins and 676 mitochondrial proteins. Ablation of USP19 led to alteration of 274 proteins, displayed as dots above the FDR curves (FDR $p = 0.05$; s0 = 0.1; Fig. 3*A* and Supplemental Table S1). Among these, the abundance of 96 proteins decreased, including the cytosol aminopeptidase (LAP3), Plastin-3 (PLS3), Ras-related protein Rab-9A (RAB9A) and, in agreement with a previous study reporting it as a direct USP19 substrate, α-synuclein (displayed by gene name SNCA, (9)) (Fig. 3*A* and Supplemental Table S1), while levels of 178 proteins increased, including the elongation factor 1-α 2 (EEF1A2), cysteine protease ATG4B

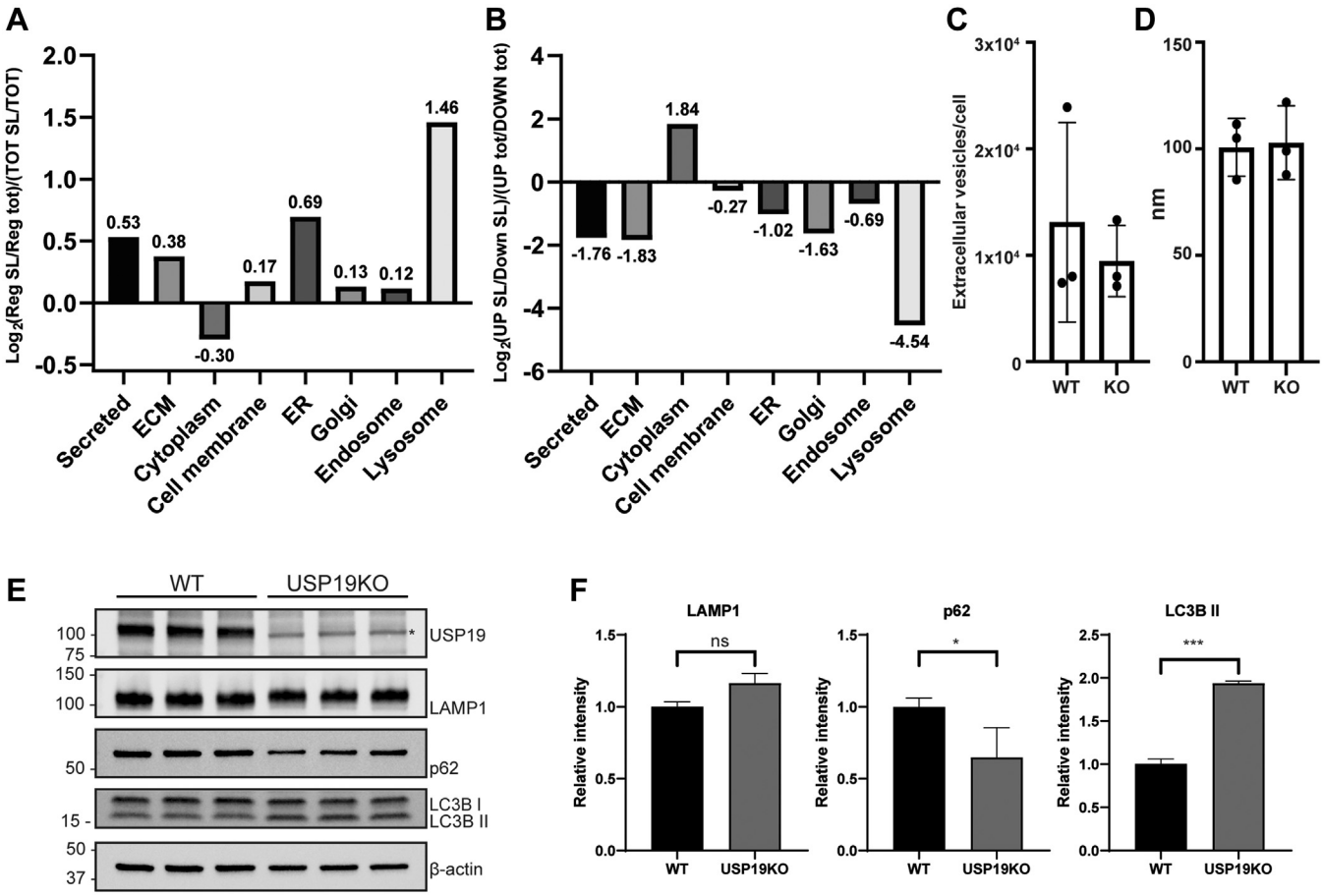

FIG. 2. **Subcellular location analysis of proteins secreted by USP19KO HEK cells**. *A*, analysis of subcellular locations among proteins regulated in USP19KO cells. For each displayed subcellular location, the ratio between the number of regulated proteins with a specific subcellular location (RegSL) and the total number of regulated proteins (RegTot) was normalized in a logarithmic scale against the ratio between the total number of proteins with a specific subcellular location (TOTSL) and the total number of proteins detected in the secretome (TOT). *B*, analysis of changes in subcellular locations among proteins regulated in USP19KO cells. For each displayed subcellular location, the ratio between the number of upregulated and downregulated proteins with a specific subcellular location (Up SL and Down SL, respectively) was normalized in a logarithmic scale against the ratio between the total number of upregulated proteins (UP tot) and downregulated proteins (Down tot). Nanoparticle Tracking Analysis of the number (*C*) and size (*D*) of extracellular vesicles released by USP19WT or KO HEK293T cells. Western blots (*E*) and relative band quantifications (*F*) of LAMP1, p62, and LC3B in the lysate of WT and USP19KO HEKs. Loss of USP19 in KO cells is also displayed (* indicates a nonspecific band that does not disappear when USP19 is ablated), and actin was used as a loading control.

(ATG4B), small glutamine-rich tetratricopeptide repeat–containing protein α (SGTA), BTB/POZ domain-containing protein KCTD12 (KCTD12), and myosin-9 (MYH9) (Fig. 3*A* and Supplemental Table S1). Unlike the result from the secretome analysis, in which more than one third of lysosomal proteins were altered, only six out 106 lysosomal proteins (about the 5%) were altered in the lysate, further underscoring the specificity for USP19-regulated lysosomal secretion (Fig. 3*C*).

Secretome and Cell Proteome Cross-Evaluation for the Identification of Proteins Secreted in an USP19-dependent Manner

To identify proteins secreted through an USP19-dependent mechanism, we performed a cross-evaluation of secretome and lysates of USP19KO HEK cells. We reasoned that proteins secreted in a USP19-dependent manner should be reduced in the secretome and accumulate, or at least not decrease, in the lysates of USP19KO cells. One thousand two hundred seventy-four proteins were identified in both conditioned media and lysates (Fig. 4*A*), of which 975 were not altered in both fractions (Fig. 4*B*). One hundred thirty one proteins increased in the conditioned media of USP19KO cells, potentially by secondary effects triggered by USP19 loss of function (Fig. 4*B*). Sixty six proteins decreased and therefore potentially secreted through a USP19-dependent mechanism. Among them, five also decreased in cell lysates (CDH2, LAP3, PGM2, PLS3, and UGGT1), suggesting these proteins being deubiquitinated by USP19 or regulated by a different unknown mechanism. By contrast, we identified 65 potentially USP19-dependent secreted proteins. Sixty

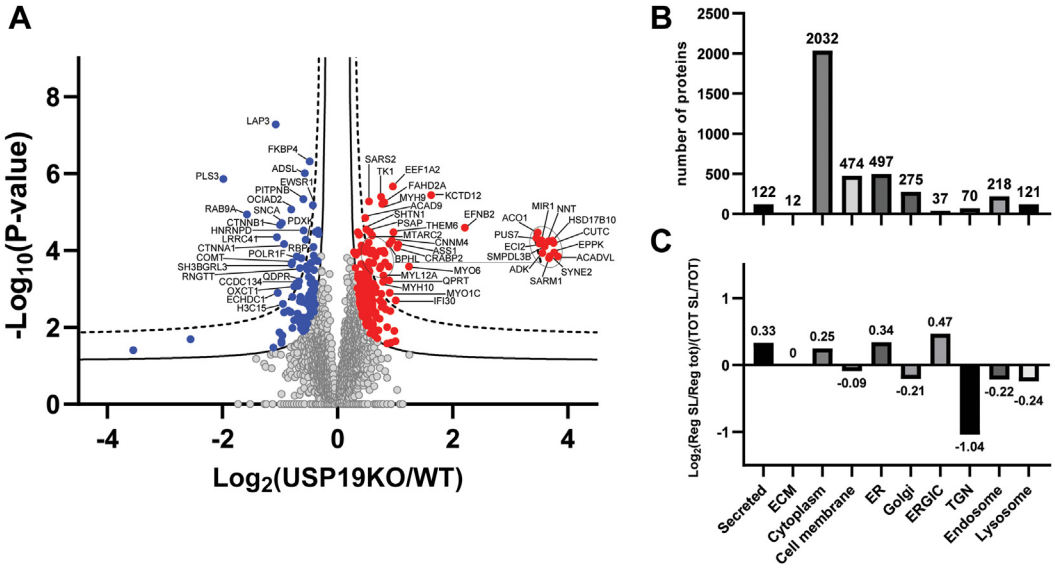

FIG. 3. **Mass spectrometry analysis of proteins differentially abundant in USP19KO cell lysate.** *A*, volcano plot showing the –Log10 of *p*-values *versus* the Log2 of protein ratio between USP19KO HEK (USP19KO) and USP19WT HEK cells of 4667 proteins (n = 6). Proteins significantly increased in USP19KO cells are displayed as *red filled dots*; proteins significantly reduced as *blue filled dots*. Unaltered proteins are displayed as the *gray dots* below the FDR, set at 0.05 (*solid lines*) and at 0.01 (*dashed lines*). Analysis of enriched subcellular locations (*B*) and changes of proteins regulated in USP19KO cells (*C*).

three of them were decreased in the conditioned media of USP19KO HEK cells and unaltered in the lysate (including several cathepsins and other lysosomal proteins). Only two proteins decreased in the conditioned media and accumulated in the lysate: a lysosomal protease, LGMN, and an ER-associated protein, thioredoxin domain-containing protein 5 (TXNDC5) (Fig. 4*B*). A GO and KEGG pathway analysis found that lysosome-associated proteins involved in the metabolism of glycolipids were the most enriched within this group (GO:0005764 - CHID1; CTSA; GRN; ASAH1; HEXB; HEXA; PLD3; CLN5; CTSL; GLB1; COL6A1; MAN2B1; CTSD; LDLR; GLA; CTSC; CTSB; TXNDC5).

USP19 Regulates Secretion of LGMN

We validated proteomics results by analysing changes in protein levels by Western blotting as an orthogonal method. First, we analyzed levels of α-synuclein (SNCA), a protein already known to undergo USP19-regulated proteasomal degradation and secretion, that our proteomic analysis found to be less abundant in the lysates of USP19KO cells (Fig. 3*A*, Supplemental Table 1) (9). Consistent with the proteomics data, immunoblotting showed that the levels of α-synuclein were decreased by 70% in the lysate of USP19KO HEK cells compared to WT controls (Fig. 5, *A* and *B*). Secreted α-synuclein was also lower in USP19KO cells (Fig. 5, *A* and *B*). However, normalizing the level of α-synuclein in conditioned media over that in cell lysate showed that reduced α-synuclein secretion in USP19KO cells can be attributed to reduced protein level in cells, suggesting that unconventional secretion of α-synuclein under serum starvation conditions may not require USP19 (21).

Next, we used immunoblotting to validate the secretion of LGMN, identified as the only lysosomal protein that decreased in the conditioned media and increased in the lysate of USP19KO cells by the mass spectrometry–based analysis (displayed by gene name LGMN in Fig. 4*B*). LGMN is synthesized as an inactive proenzyme and then targeted *via* the ER and Golgi to the endolysosomal system, where the shift to a more acidic pH induces the protease activation by an autocatalytic mechanism (the mature active form of LGMN is also referred to as the asparaginyl-specific endopeptidase; (26)). Immunoblot analysis showed that within the cell, LGMN was mainly found as its 36 kDa mature form, while in the conditioned media, the protease was found as its inactive zymogen of 56 kDa, in agreement with previous reports (27). To note, serum depletion did not affect maturation of intracellular LGMN, as shown in Supplemental Fig. S1, *A* and *B*. Extracellular levels of LGMN diminished when USP19 was ablated, while its levels in the cell lysate slightly increased, in agreement with the proteomics results (Fig. 5, *C* and *D*). Additional immunoblotting experiments showed that the, levels of two other lysosomal proteins, cathepsin D and B, were reduced in the conditioned media of USP19KO cells but their levels remained unaltered in cell lysates, indicating that, similar to LGMN and in agreement with the mass spectrometry data, their secretion was regulated by USP19 (Fig. 5, *E–H*).

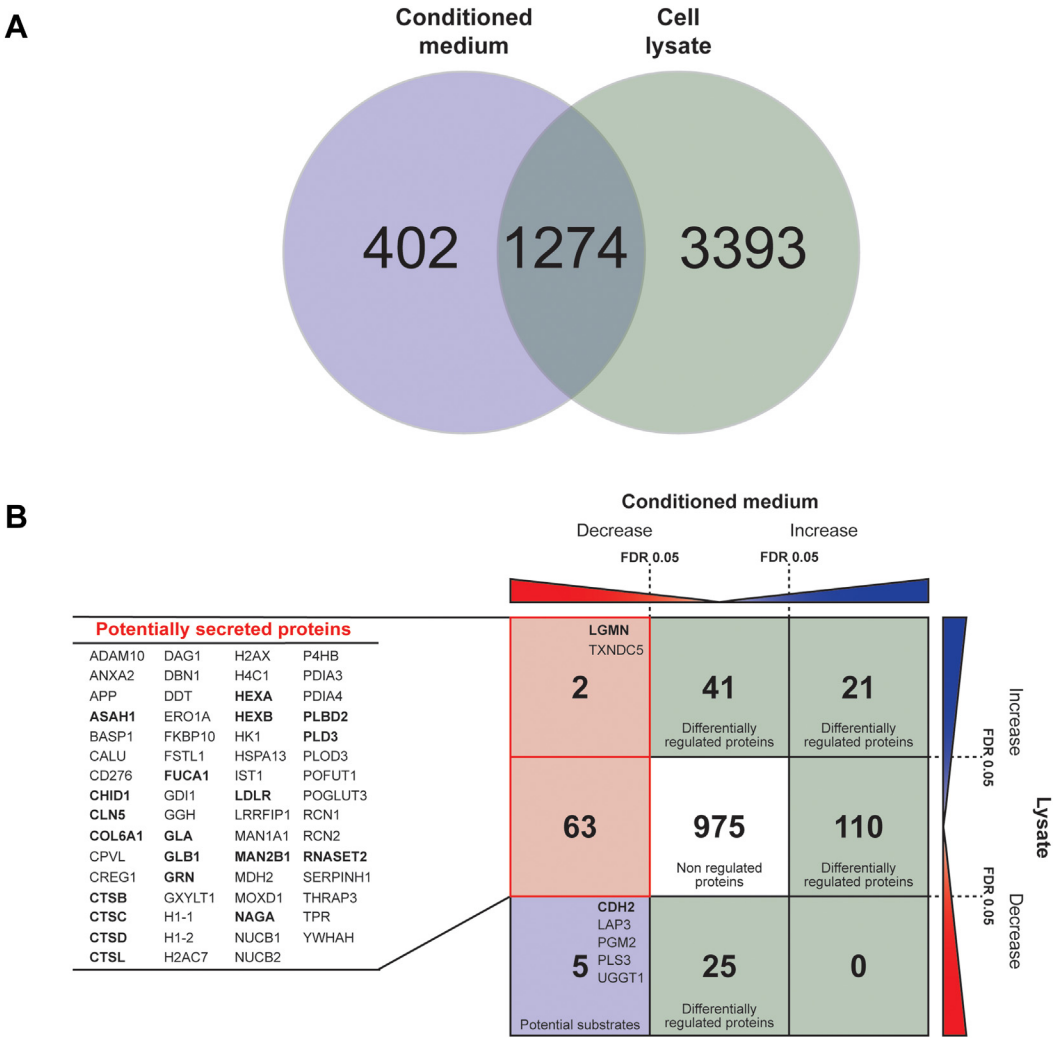

FIG. 4. **Quantitative proteomics identifies proteins secreted in a USP19-dependent manner.** *A*, Venn diagram showing the number of proteins identified by mass spectrometry analysis in the conditioned media and/or lysates of USP19KO cells. *B*, graphic representation of protein changes of the 1274 proteins identified in both conditioned media and lysates of USP19KO cells. Proteins have been divided in nine subgroups based on their increase or decrease in the conditioned media and lysates of USP19KO cells. Proteins decreased in the conditioned media and not reduced in the cell lysate (proteins potentially secreted in a USP19-dependent manner) are listed, with lysosome-resident proteins written in *bold* (according to UniProt annotation - GO 0005764)

USP19 Regulates Secretion of LGMN in Different Cell Types

Proteomics and Western blotting pinpointed LGMN as a protein secreted by a mechanism that involves USP19. Thus, we continued investigating its secretion to dissect the mechanism by which USP19 ablation impaired the release of lysosomal proteins. First, we demonstrated that ectopic expression of USP19 rescued the reduced levels of extracellular LGMN in USP19KO HEK cells (Fig. 6, *A* and *B*). Then, we silenced the expression of USP19 in a number of different cell types, including HTB94 fibroblast-like, HeLa cervical cancer and U251 human glioblastoma cells and LX-2 hepatic stellate, and analyzed the secretion of LGMN. Knockdown of USP19 in all these cell lines reduced extracellular levels of LGMN, without affecting their levels in the lysates (Fig. 6, *C–F*). Altogether these data suggested that LGMN secretion is regulated by USP19 in a variety of cell types in addition to HEKs (Fig. 6).

USP19 Regulation of LGMN Secretion Requires Autophagosome Formation

After having validated LGMN as a protein whose secretion is regulated by USP19, we dissected the molecular mechanism underlaying this process by using protein-trafficking inhibitors. Brefeldin A (BFA), which blocks the ER to Golgi transport, largely reduced levels of LGMN in the conditioned media of WT and USP19KO cells (Fig. 7, *A* and *B*). In the lysates of untreated cells, LGMN mostly appeared as a band below 37 kDa corresponding to the active form of the protease

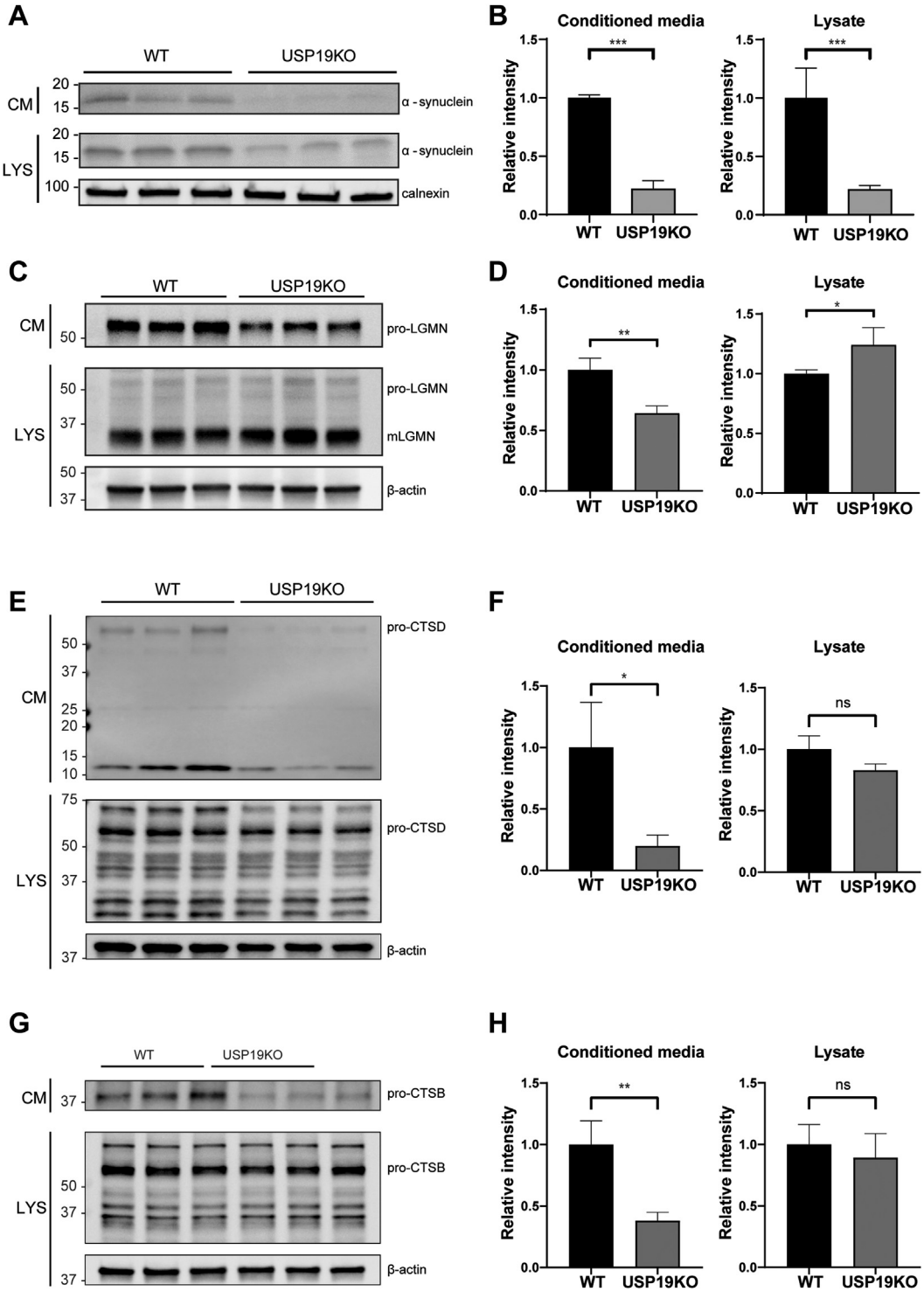

FIG. 5. **Orthogonal validation of proteins with decreased levels in the secretome of USP19KO cells.** *A–H*, immunoblots showing protein abundance and relative densitometric quantifications of α-synuclein (*A* and *B*), legumain (LGMN) (*C* and *D*), cathepsin D (CTSD) (*E* and *F*), and cathepsin B (CTSB) (*G* and *H*) in the conditioned media and lysates of WT or USP19KO HEK cells (densitometric quantifications shown as mean values ± SD; * represents $p < 0.05$, ** represents $p < 0.01$, and *** represents $p < 0.005$, Student's *t* test; three independent experiments are displayed out of six quantified, n = 6). To note, an uncropped image of blots in (*C*) is shown in the Supplemental Fig. S2*A*.

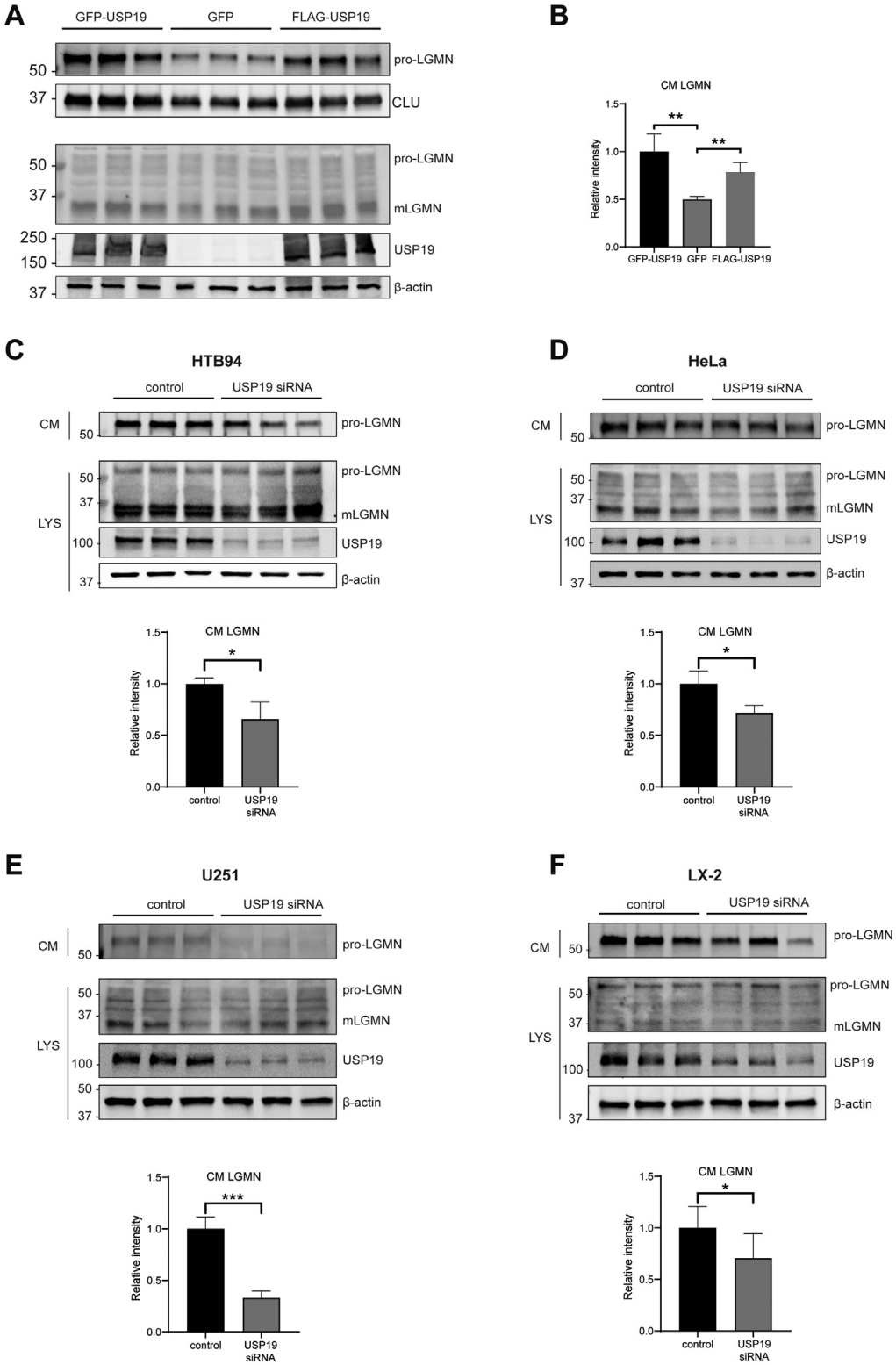

FIG. 6. **USP19 regulates the secretion of LGMN in different cell types.** *A* and *B*, immunoblots showing protein abundance (*A*) and relative densitometric quantifications (*B*) of LGMN in the conditioned media and lysates of USP19KO HEK cells, transfected either with GFP-USP19, GFP, or FLAG-USP19. Expression of USP19 in the KO cells increased levels of LGMN in the conditioned media compared to GFP expressing control cells, indicating that ectopic expression of USP19 rescued secretion of the two proteins (densitometric quantifications shown as mean values ± SD; ** represents $p < 0.01$, Student's *t* test; three independent experiments are displayed out of six quantified, n = 6). Clusterin

(mLGMN) regardless of USP19 depletion. BFA caused reduction in the levels of such a mature form of LGMN and led to the increase of a band above 50 kDa corresponding to the immature pro-form of LGMN (pro-LGMN), indicating that BFA led to an accumulation of its zymogene within the cell by preventing the protease to reach the lysosome and therefore getting activated. Overall effects of BFA were quite similar in USP19KO and WT cells. 3-MA, an inhibitor of PI3K frequently used to block autophagy, reduced the extracellular levels of LGMN in WT and USP19KO cells (Fig. 7, *C* and *D*). In addition, 3-MA inhibited full activation of LGMN, resulting in a form of slightly higher molecular weight in the lysate of both cell types, compatible with an active intermediate of the protein (26). Altogether, 3-MA had comparable effects on the secretion of LGMN in WT and USP19KO cells. Chloroquine, which increases the intravesicular pH and impairs autophagosome fusion with lysosomes, inhibited the pH-dependent activation of LGMN (*i.e.* the band below 37 kDa corresponding to the mature form of the protease almost disappeared and the band above 50 kDa corresponding to its immature form accumulated) and enhanced its secretion into the conditioned media (Fig. 7, *E* and *F*). Intriguingly, chloroquine rescued diminished secretion of LGMN in USP19KO cells. GW4869 is a frequently used inhibitor of ceramide-modulated inward budding of multivesicular bodies and subsequent exosome release (28). GW4869 increased LGMN secretion in WT cells and rescued its decrease secretion in USP19KO cells, while it did not lead to evident effects on the maturation of intracellular LGMN (Fig. 7, *G* and *H*). This indicated that USP19-dependent secretion of LGMN could occur through a mechanism divergent from exosome release, but with it dynamically interconnected as it was enhanced by blockade of exosome formation. Dynasore, which is an inhibitor of dynamin activity, prevents fission and recycling of endocytic endosomes (29). Dynasore reduced extracellular levels of LGMN in WT cells, while its effects were minimal in USP19KO cells (Fig. 7, *I* and *L*). Differently from 3-MA and chloroquine, Dynasore did not affect maturation of LGMN as the protein was mainly present in its mature form in the lysate of both WT and USP19KO cells. However, levels of intracellular LGMN were reduced of about 40% in Dynasore-treated cells, suggesting that the inhibitor affected its stability rather than its secretion. Altogether, these data suggested that the USP19-dependent secretion of LGMN could occur through a mechanism opposite to exosome release that required PI3K and the fusion of intracellular pH-sensitive vesicles with the plasma membrane.

USP19 Regulates Secretion of LGMN and the Other Lysosomal Proteins by a Mechanism Independent from Their Direct Interaction

Next, we investigated whether USP19 regulated the secretion of LGMN and the other lysosomal proteins through a direct interaction. To do this, FLAG-tagged USP19 (or a FLAG-tagged control protein – matrix remodeling associated 8, MXRA8) was expressed in HEK cells, immunoprecipitated from cell extracts with an anti-FLAG resin, and proteins co-immunoprecipitated with USP19 analyzed by immunoblotting and proteomics. USP19 co-immunoprecipitated with HSP90, a known interactor of the protein (30), but not with LGMN (Fig. 8*A*). Then, immunoprecipitates were applied to unbiased high-resolution mass spectrometry, and the relative abundance of proteins co-immunoprecipitated with USP19-FLAG was compared to that of proteins co-immunoprecipitated with the FLAG-tagged control protein. The analysis identified 5208 proteins. As expected, USP19 was the most abundant protein in the USP19-FLAG immunoprecipitates and MXRA8 in the controls (Fig. 8*B*). A number of HSP90 subunits (such as HSP90AA1 and HSP90AB1) co-immunoprecipitated with USP19, in agreement with our immunoblotting results and previous reports (30). The analysis identified a number of putative interactors of USP19, such as the Golgi-associated PDZ and coiled-coil motif-containing protein (GOPC), Xaa-Pro aminopeptidase 3 (XPNPEP3), neuralized-like protein 4 (NEURL4), and E3 ubiquitin-protein ligase HERC2 (Fig. 6*F*). Conversely, LGMN, cathepsin B, C, D, and L did not interact with USP19 compared to the FLAG-tagged control protein, alike the large majority of the proteins whose secretion was impaired in USP19KO cells (Supplemental Fig. S1, *D* and *E* and Supplemental Table S2). Altogether, these results indicate that USP19 regulates the secretion of LGMN, cathepsins, and other lysosomal proteins by a mechanism that does not involve their direct interaction.

Secretion of Lysosomal Proteins are Not DUB Substrate of USP19

Both proteomics and Western blotting found that intracellular levels of LGMN and other lysosomal proteins, such as cathepsins, were not reduced in the lysate of USP19KO cells, suggesting that altered secretion of these proteins did not depend on their deubiquitination by USP19 and subsequential augmented proteasomal degradation. To confirm this, we treated USP19KO and WT cells with the proteasome inhibitor MG132, and then we isolated ubiquitinated proteins by Ubi-Qapture and analyzed them by immunoblotting and

was used as an example of protein that is secreted into the conditioned media independently from USP19. Levels of USP19 in the lysate of transfected cells are displayed, together with actin that was used as a loading control. *C–F*, immunoblots and their relative band densitometric quantifications showing LGMN in USP19 knockdown or control HTB94 (*C*), HeLa (*D*) U251 (*E*), and LX-2 cells (*F*). For each cell type, levels of USP19 in the lysate were shown. Actin was used as a loading control. USP19 silencing in these cells led to a decrease of LGMN in the conditioned media, while it did not alter its cellular levels (densitometric quantifications shown as mean values ± SD; * represents $p < 0.05$; ** represents $p < 0.01$; and *** represents $p < 0.005$, Student's *t* test; three independent experiments are displayed out of six quantified, n = 6).

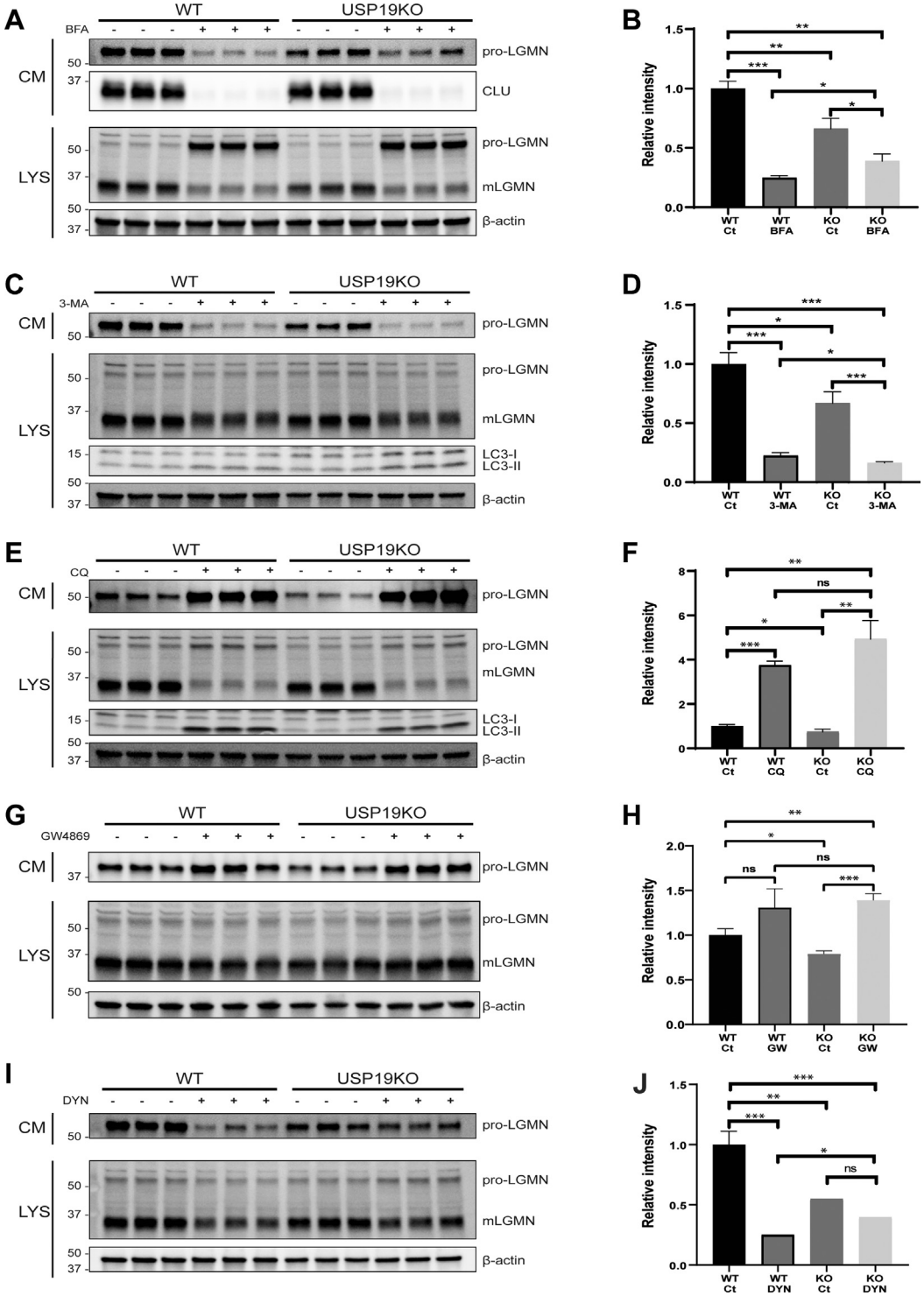

FIG. 7. **LGMN is secreted through an USP19-dependent mechanism that requires PI3K and the fusion of intracellular pH sensitive vesicles with the plasma membrane**. Immunoblots showing protein abundance and relative densitometric quantifications of LGMN in the conditioned media and cell lysates of WT and USP19KO HEK cells, treated with or without 350 nM brefeldin A (BFA) (*A* and *B*), 10 mM 3-methyladenosine (3-MA) (*C* and *D*) or 10 nM chloroquine (CQ) (*E* and *F*), 10 μM GW4869 (*G* and *H*), and 80 μM dynasore for 24 h (I-J). Clusterin (CLU), a protein known to be secreted in a conventional manner, was used to show effectiveness of the BFA treatment and actin was used as a loading control in (*A*). LC3-I to LC3-II conversion was observed in 3-MA–treated cells to confirm reduction in autophagosome formation in the presence of the inhibitor, and actin was used as a loading control in (*C*). LC3-I to LC3-II conversion was analysed to confirm inhibition of lysosomal activity in the presence of CQ, and actin was used as a loading control in (*E*).

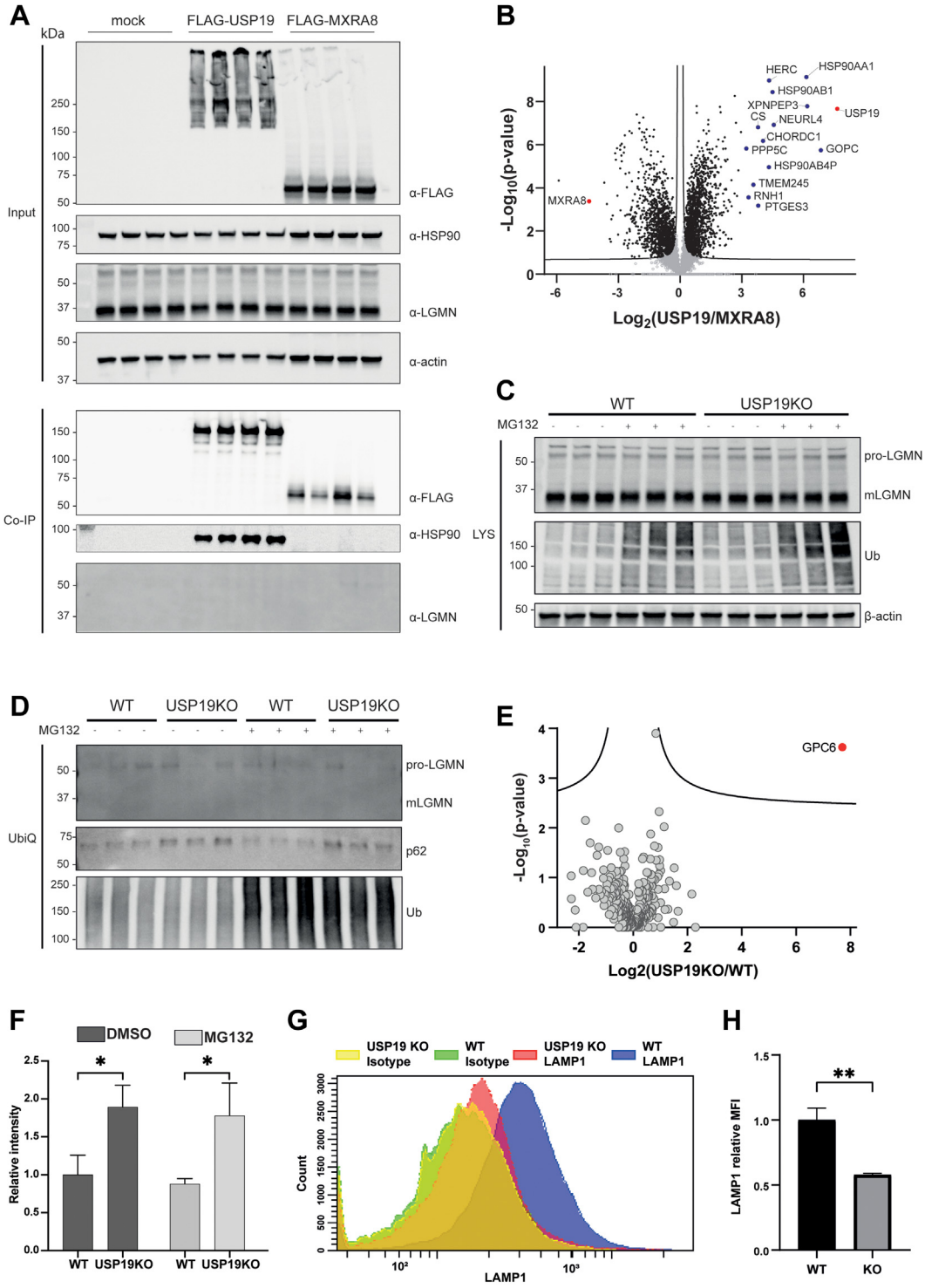

FIG. 8. **Secretion of lysosomal proteins is not regulated by their deubiquitination by USP19 or direct interaction with the DUB.** *A*, cell lysates and immunoprecipitates from HEK cells transfected with USP19-FLAG, MXRA8-FLAG, or an empty vector were immunoblotted for LGMN and the known USP19 interactor HSP90. β-actin was used as a loading control. *B*, volcano plot showing the –Log10 of *p*-values *versus* the Log2 of protein ratio of 5208 proteins between the immunoprecipitates from USP19-FLAG– and FLAG-MXRA8–transfected HEK cells. USP19 and MXRA8 are displayed as filled *red* dots. Significantly altered proteins (*i.e.* proteins above the FDR curves) are displayed as filled *black dots*, and those with a Log2 USP19/MXRA8 ratio above 3 (putative USP19 interactors) are displayed with *blue dots*. Not altered proteins are displayed as *open gray* circles. *C*, immunoblots showing LGMN in WT and USP19KO HEKs, in the presence or absence of the proteasome inhibitor MG132. Ubiquitin (Ub) was used as a control for MG132 treatment, and β-actin as a loading control. *D* and *E*, ubiquitinated proteins

proteomics. MG132 did not alter intracellular levels of LGMN in both USP19KO and WT cells (Fig. 8*C*). Only a minimal part of intracellular LGMN was ubiquitinated, and its levels were similar in USP19KO and WT cells, either treated or not with MG132 (Fig. 8, *D* and *E*).

Next, we analyzed ubiquitinated proteins isolated from USP19KO and WT cells, treated with MG132 to avoid their proteasomal degradation, with high-resolution mass spectrometry to identify DUB substrates of USP19. The analysis identified 460 proteins isolated from both USP19KO and WT cells (Fig. 8*F* and Supplemental Table S3 to note, in the absence of MG132 only 91 proteins were detected). Only one protein, glypican 6 (GPC6), was significantly more abundant in USP19KO cells, suggesting it as a possible substrate of USP19 (Fig. 8*F*). Among proteins whose secretion was impaired by loss of USP19, only CTSD, ANXA2 and H1-2 were identified within this dataset, but none of these proteins was differentially ubiquitinated (Fig. 8*F* and Supplemental Fig. S1*C*). All other proteins with reduced secretion were not found in this analysis, suggesting their little or no ubiquitination.

It has been reported that cathepsins and other lysosomal hydrolases (*e.g.* hexosaminidase A and B) can be released by "lysosomal exocytosis", a process leading to their secretion upon lysosome fusion with the plasma membrane (31–33). p62 plays a crucial role in this process, as it bridges the interaction between lysosomal vesicles and the ER when in its mono-ubiquitinated form. USP15 and USP17 promote lysosomal exocytosis of lysosomal proteins, including cathepsin D and LGMN, by deubiquitinating p62. This event allows the release of lysosomal vesicles from the ER and their trafficking to the plasma membrane (34–36). Thus, we investigated whether USP19, similar to USP15 and USP17, could deubiquitinate p62. Despite total levels of p62 were lower in USP19KO cells (Fig. 2*E*), ubiquitinated p62 was clearly increased when USP19 was ablated (Fig. 8, *D* and *F*). When lysosomes fuse with the plasma membrane, epitopes present on the luminal domain of LAMP1 are exposed on the cell surface and their detection on unpermeabilized cells is a general method to investigate lysosomal exocytosis (37). In agreement with our hypothesis, we found that levels of LAMP1 on the cell surface of USP19KO cells were reduced compared to WT cells (Fig. 8, *G* and *I*). Altogether, these data suggest that rather than controlling the release of LGMN, cathepsins and the other lysosomal proteins through their direct deubiquitination, USP19 could regulate their secretion *via* an indirectly mechanism (See Discussion).

DISCUSSION

USP19 is a multifunctional protein that has emerged to play a crucial role in a number of biological processes, including immune responses to viruses and cell migration, for its ability to deubiquitinate specific proteins and prevent them from proteasomal degradation (4, 6, 9, 38, 39). Interestingly, USP19 was also found to interact with HSP90 and HSC70, two most abundant chaperones that sense unfolded proteins, and play a crucial role in the unconventional secretion of misfolded proteins (30). In this study, we applied USP19KO HEK293T cells to a workflow for secretome analysis to identify proteins whose secretion is regulated by USP19. Our study indeed suggests a critical regulatory function for USP19 in unconventional protein secretion. Intriguingly, loss of USP19 most significantly diminished levels of lysosomal proteins in the conditioned media, without significantly altering their levels in the lysate. Such proteins, including LGMN and a number of cathepsins, were secreted by a mechanism that is regulated by USP19 and did not involve extracellular vesicles, as USP19 knockout did not affect the number and size of extracellular vesicles. Notably, several lines of evidence suggest that LGMN secretion occurs *via* a mechanism more akin to a specialized form of unconventional protein secretion dubbed as lysosomal exocytosis. First, the secretion of LGMN is inhibited by 3-MA, a PI3K inhibitor often used to block autophagosome formation and its fusion with lysosomes. Second, LGMN secretion was significantly enhanced by chloroquine, a known stimulator of autophagic/lysosomal secretion (40). Cathepsins and other lysosome-resident hydrolases are known to be released by a similar mechanism, further supporting the hypothesis that USP19 could regulate lysosomal exocytosis and therefore the release of lysosomal proteins in the extracellular milieu (31–33). Furthermore, this hypothesis is in line with the recently identified role of another deubiquitinase, USP17, in regulating the peripheral trafficking of lysosomes and release of lysosomal proteases (34). At the steady-state, lysosomes are tethered to the ER *via* the ER-resident E3 ligase RNF26, which ubiquitinates p62 allowing it to act as a bridge between the ER and lysosomes, as it is recognized by ubiquitin-binding domains (UBDs) of lysosomal vesicles adaptors. Upon stimulation with cytokines or growth

enriched from WT and USP19KO cells, treated with or without MG132, were analyzed by immunoblotting and unbiased proteomics. *D*, immunoblots showing ubiquitinated LGMN and p62 in WT and USP19KO HEKs, either in the presence or absence of MG132. *E*, volcano plots showing the −Log10 of *p*-values *versus* the Log2 of protein ratio between USP19KO and WT cells, treated with MG132 to inhibit proteasomal degradation, of 460 proteins (n = 3). Glypican 6 (GPC6) was the only significantly regulated protein and it is displayed as a *red* filled dot above the FDR (*black hyperbolic curves*). Not altered proteins are displayed as *gray* dots below the FDR. *F*, quantification of p62 bands from the immunoblot shown in (*D*) (n = 3; * represents $p < 0.05$; Student's *t* test). *G* and *H*, flow cytometry analysis shows that levels of LAMP1 on the cell surface of WT HEKs were higher than on USP19KO HEKs. Flow cytometry histograms are shown in (*G*), and quantification of three separate experiments in (*H*) (** represents $p < 0.01$, Student *t* test).

factors, USP17 is induced and it deubiquitinates p62, thereby releasing the lysosomes from the ER and facilitating their trafficking to the plasma membrane (34). Similarly, USP15 can also deubiquitinate p62, opposing RFN26 and allowing vesicle release into the cell's periphery (35). We found that loss of USP19 increased the levels of ubiquitinated p62 and reduced lysosomal exocytosis under serum starvation condition, suggesting that USP19 may regulate lysosomal exocytosis by a similar mechanism. We postulate that these DUBs may regulate lysosomal secretion under different conditions. Whether these enzymes have overlapping roles in lysosome exocytosis remains to be determined.

The endo-lysosomal system is strictly interconnected with the autophagic system (41). Autophagy is a cellular process leading to sequestration of cytosolic cargoes for their degradation within lysosomes. However, the autophagic machinery is also involved in the unconventional secretion of proteins, as it can target cargo proteins to the plasma membrane for secretion, rather than to the lysosomes for degradation (42). This pathway, known as secretory autophagy, has been described as associated with stress-induced autophagy. Secretory autophagy is stimulated by cell starvation, and it regulates unconventional secretion of a number of leaderless proteins, including IL-1β and α-synuclein (43, 44). Secretome analysis of starved murine macrophages, in which secretory autophagy was impaired by ablation of autophagy protein 5 (ATG5), showed reduced release of several proteins whose release was also impaired by USP19 loss, including cathepsins (CTSB, CTSC, CTSD), lysosomal enzymes (β-hexosaminidase - HEXA, HEXB - alpha-N-acetylgalactosaminidase - NAGA) and others (45). Furthermore, our results showed that LGMN secretion is sensitive to BFA and that secreted LGNM is mostly in an unprocessed inactive form, strongly indicating that LGMN secretion is likely initiated from a pre-lysosomal compartment derived from the Golgi. This evidence suggests that USP19 could function at the intersection between the endo-lysosomal system and the autophagic system. In the future, it would be interesting to investigate where lysosomal exocytosis and secretory autophagy diverge, and whether different DUBs can regulate the release of different vesicles throughout the autophagosome-lysosome axis.

USP19 knockout mice display a number of phenotypes, further suggesting the functional complexity and substrate diversity of the protein. Reported studies showed that USP19 can either stabilize proteins, which are degraded more efficiently by the proteasome when the enzyme is ablated, or target substrates to lysosomes and intracellular vesicles for degradation or secretion. Our analysis found 96 proteins that are decreased in the lysate of USP19KO cells, and 178 proteins that are increased. Decreased proteins, including LAP3, PLS3 and OCIAD2, could be substrates of the deubiquitinating activity of USP19 (although they were not identified within our proteomic dataset of ubiquitinated proteins), which may be degraded at higher rate by the ubiquitin-proteome system when USP19 is ablated. On the contrary, proteins that increased in USP19KO cells may be proteins that are targeted for lysosomal degradation by USP19- and DNAJC5-dependent endosome microautophagy or other forms of autophagy that depend on the interaction between USP19 and beclin one under starvation conditions (8). Although the experimental set-up reported here is particularly suited to comparing secretomes of cells with different genetic backgrounds and analyse how loss of a specific protein affects the secretome composition, our study relies on studying cells cultured in the absence of serum for technical constraints. Indeed, even the most updated mass spectrometers have a limit of ions that can be detected during the analysis, and therefore high abundant serum proteins tend to cover the signals of less abundant proteins in a biological sample (46). This method may favour the identification lysosomal/autophagic secretion cargoes because serum starvation is known to trigger autophagy (47). By contrast, USP19-mediated MAPS, which is restricted by serum starvation, may largely escape our detection, which requires future elucidation with improved methodology.

In conclusion, we applied an innovative workflow of secretome analysis to consolidate a previously underappreciated role of USP19 autophagic/lysosomal secretion. Additionally, complementary proteomic analyses allowed identification of lysosomal proteins whose secretion is regulated by this multifunctional protein by a mechanism resembling the p62-mediated lysosomal exocytosis.

DATA AVAILABILITY

Proteomic data have been deposited to the ProteomeXchange Consortium *via* the PRIDE partner repository with the following dataset identifiers:

- Analysis of USP19KO and WT cell secretome and proteome: PXD055064 and 10.6019/PXD055064;
- USP19 interactomics: PXD055081.
- Analysis of enriched ubiquitinated proteins from USP19KO and WT cells: PXD055118.

The annotated MS/MS spectra from the MaxQuant dataset can be viewed *via* MS-Viewer by entering the key "okiubbketm" MS-Viewer Report (ucsf.edu).

Supplemental data—This article contains supplemental data.

Funding and additional information—This work was funded by the Deutsche Forschungsgemeinschaft (DFG, German Research Foundation) under Germany's Excellence Strategy within the framework of the Munich Cluster for Systems Neurology (EXC 2145 SyNergy– ID 390857198).

Author contributions—S. B. and S. D. C. writing–original draft; S. B. and M. L. P. investigation; Y. Y., S. A. M., and S.

F. L. writing–review and editing; Y. Y. resources; S. A. M. formal analysis; S. F. L. and S. D. C. supervision; S. D. C. project administration; S. D. C. conceptualization.

Conflicts of interest—The authors declare that they have no conflicts of interests with the contents of this article.

Abbreviations—The abbreviations used are: 3-MA, 3-methyladenine; AGC, automatic gain control; BFA, Brefeldin A; CUPS, compartment of unconventional protein secretion; DIA, data-independent acquisition; DUB, deubiquitinating enzyme; ECM, extracellular matrix; ER, endoplasmic reticulum; HEK, human embryonic kidney 293T; KEGG, Kyoto Encyclopedia of Genes and Genomes; LFQ, label-free quantification; LGMN, legumain; MAPS, misfolding-associated protein secretion; UPS, ubiquitin-proteasome system; USP19, ubiquitin carboxyl-terminal hydrolase 19.

Received April 8, 2024, and in revised form, September 26, 2024
Published, MCPRO Papers in Press, October 9, 2024, https://doi.org/10.1016/j.mcpro.2024.100854

REFERENCES

1. Ciechanover, A. (2015) The unravelling of the ubiquitin system. *Nat. Rev. Mol. Cell Biol.* **16**, 322–324
2. Nandi, D., Tahiliani, P., Kumar, A., and Chandu, D. (2006) The ubiquitin-proteasome system. *J. Biosci.* **31**, 137–155
3. Hassink, G. C., Zhao, B., Sompallae, R., Altun, M., Gastaldello, S., Zinin, N. V., *et al*. (2009) The ER-resident ubiquitin-specific protease 19 participates in the UPR and rescues ERAD substrates. *EMBO Rep.* **10**, 755–761
4. Lei, C. Q., Wu, X., Zhong, X., Jiang, L., Zhong, B., and Shu, H. B. (2019) USP19 inhibits TNF-alpha- and IL-1beta-triggered NF-kappaB activation by deubiquitinating TAK1. *J. Immunol.* **203**, 259–268
5. Zhang, J., Bouch, R. J., Blekhman, M. G., and He, Z. (2021) USP19 suppresses Th17-driven pathogenesis in autoimmunity. *J. Immunol.* **207**, 23–33
6. Zhao, X., Di, Q., Yu, J., Quan, J., Xiao, Y., Zhu, H., *et al*. (2021) USP19 (ubiquitin specific peptidase 19) promotes TBK1 (TANK-binding kinase 1) degradation *via* chaperone-mediated autophagy. *Autophagy* **18**, 891–908
7. Cui, J., Jin, S., and Wang, R. F. (2016) The BECN1-USP19 axis plays a role in the crosstalk between autophagy and antiviral immune responses. *Autophagy* **12**, 1210–1211
8. [preprint] Lee, J., Xu, Y., Saidi, L., Xu, M., Zinsmaier, K., and Ye, Y. (2021) Abnormal triaging of misfolded proteins by adult neuronal ceroid lipofuscinosis-associated CSPα mutants causes lipofuscin accumulation. *bioRxiv*. https://doi.org/10.1101/2021.07.16.452648
9. Lee, J. G., Takahama, S., Zhang, G., Tomarev, S. I., and Ye, Y. (2016) Unconventional secretion of misfolded proteins promotes adaptation to proteasome dysfunction in mammalian cells. *Nat. Cell Biol.* **18**, 765–776
10. Malhotra, V. (2013) Unconventional protein secretion: an evolving mechanism. *EMBO J.* **32**, 1660–1664
11. Xu, Y., Cui, L., Dibello, A., Wang, L., Lee, J., Saidi, L., *et al*. (2018) DNAJC5 facilitates USP19-dependent unconventional secretion of misfolded cytosolic proteins. *Cell Discov.* **4**, 11
12. Fontaine, S. N., Zheng, D., Sabbagh, J. J., Martin, M. D., Chaput, D., Darling, A., *et al*. (2016) DnaJ/Hsc70 chaperone complexes control the extracellular release of neurodegenerative-associated proteins. *EMBO J.* **35**, 1537–1549
13. Wisniewski, J. R., Zougman, A., Nagaraj, N., and Mann, M. (2009) Universal sample preparation method for proteome analysis. *Nat. Methods* **6**, 359–362
14. Rappsilber, J., Ishihama, Y., and Mann, M. (2003) Stop and go extraction tips for matrix-assisted laser desorption/ionization, nanoelectrospray, and LC/MS sample pretreatment in proteomics. *Anal. Chem.* **75**, 663–670
15. Scilabra, S. D., Pigoni, M., Pravata, V., Schatzl, T., Muller, S. A., Troeberg, L., *et al*. (2018) Increased TIMP-3 expression alters the cellular secretome through dual inhibition of the metalloprotease ADAM10 and ligand-binding of the LRP-1 receptor. *Sci. Rep.* **8**, 14697
16. Chen, E. Y., Tan, C. M., Kou, Y., Duan, Q., Wang, Z., Meirelles, G. V., *et al*. (2013) Enrichr: interactive and collaborative HTML5 gene list enrichment analysis tool. *BMC Bioinform.* **14**, 128
17. Team, R. (2020) *RStudio: integrated development for R*. RStudio, PBC, Boston, MA
18. Thery, C., Amigorena, S., Raposo, G., and Clayton, A. (2006) Isolation and characterization of exosomes from cell culture supernatants and biological fluids. *Curr. Protoc. Cell Biol.* https://doi.org/10.1002/0471143030.cb0322s30
19. Shevchenko, A., Tomas, H., Havlis, J., Olsen, J. V., and Mann, M. (2006) In-gel digestion for mass spectrometric characterization of proteins and proteomes. *Nat. Protoc.* **1**, 2856–2860
20. Meissner, F., Scheltema, R. A., Mollenkopf, H. J., and Mann, M. (2013) Direct proteomic quantification of the secretome of activated immune cells. *Science* **340**, 475–478
21. Lee, J., Xu, Y., Zhang, T., Cui, L., Saidi, L., and Ye, Y. (2018) Secretion of misfolded cytosolic proteins from mammalian cells is independent of chaperone-mediated autophagy. *J. Biol. Chem.* **293**, 14359–14370
22. Xie, Z., Bailey, A., Kuleshov, M. V., Clarke, D. J. B., Evangelista, J. E., Jenkins, S. L., *et al*. (2021) Gene set knowledge discovery with Enrichr. *Curr. Protoc.* **1**, e90
23. Rabouille, C. (2017) Pathways of unconventional protein secretion. *Trends Cell Biol.* **27**, 230–240
24. Li, J., Deffieu, M. S., Lee, P. L., Saha, P., and Pfeffer, S. R. (2015) Glycosylation inhibition reduces cholesterol accumulation in NPC1 protein-deficient cells. *Proc. Natl. Acad. Sci. U. S. A.* **112**, 14876–14881
25. Jiang, P., and Mizushima, N. (2015) LC3- and p62-based biochemical methods for the analysis of autophagy progression in mammalian cells. *Methods* **75**, 13–18
26. Dall, E., and Brandstetter, H. (2016) Structure and function of legumain in health and disease. *Biochimie* **122**, 126–150
27. Jafari, A., Qanie, D., Andersen, T. L., Zhang, Y., Chen, L., Postert, B., *et al*. (2017) Legumain regulates differentiation fate of human bone marrow stromal cells and is altered in postmenopausal osteoporosis. *Stem Cell Rep.* **8**, 373–386
28. Catalano, M., and O'Driscoll, L. (2020) Inhibiting extracellular vesicles formation and release: a review of EV inhibitors. *J. Extracell. Vesicles* **9**, 1703244
29. Macia, E., Ehrlich, M., Massol, R., Boucrot, E., Brunner, C., and Kirchhausen, T. (2006) Dynasore, a cell-permeable inhibitor of dynamin. *Dev. Cell* **10**, 839–850
30. Lee, J.-G., Kim, W., Gygi, S., and Ye, Y. (2014) Characterization of the deubiquitinating activity of USP19 and its role in endoplasmic reticulum-associated degradation*. *J. Biol. Chem.* **289**, 3510–3517
31. Tancini, B., Buratta, S., Delo, F., Sagini, K., Chiaradia, E., Pellegrino, R. M., *et al*. (2020) Lysosomal exocytosis: the extracellular role of an intracellular organelle. *Membranes (Basel)* **10**, 406
32. Castro-Gomes, T., Corrotte, M., Tam, C., and Andrews, N. W. (2016) Plasma membrane repair is regulated extracellularly by proteases released from lysosomes. *PLoS One* **11**, e0152583
33. Rodríguez, A., Webster, P., Ortego, J., and Andrews, N. W. (1997) Lysosomes behave as Ca2+-regulated exocytic vesicles in fibroblasts and epithelial cells. *J. Cell Biol.* **137**, 93–104
34. Lin, J., McCann, A. P., Sereesongsaeng, N., Burden, J. M., Alsa'd, A. A., Burden, R. E., *et al*. (2022) USP17 is required for peripheral trafficking of lysosomes. *EMBO Rep.* **23**, e51932
35. Jongsma, M. L. M., Berlin, I., Wijdeven, R. H. M., Janssen, L., Janssen, G. M. C., Garstka, M. A., *et al*. (2016) An ER-associated pathway defines endosomal architecture for controlled cargo. *Transport Cell* **166**, 152–166
36. Bonifacino, J. S., and Neefjes, J. (2017) Moving and positioning the endolysosomal system Current. *Opin. Cell Biol.* **47**, 1–8
37. Andrews, N. W. (2017) Detection of lysosomal exocytosis by surface exposure of Lamp1 luminal epitopes. *Methods Mol. Biol.* **1594**, 205–211
38. Rossi, F. A., Enrique Steinberg, J. H., Calvo Roitberg, E. H., Joshi, M. U., Pandey, A., Abba, M. C., *et al*. (2021) USP19 modulates cancer cell migration and invasion and acts as a novel prognostic marker in patients with early breast cancer. *Oncogenesis* **10**, 28
39. Jin, S., Tian, S., Chen, Y., Zhang, C., Xie, W., Xia, X., *et al*. (2016) USP19 modulates autophagy and antiviral immune responses by deubiquitinating Beclin-1. *EMBO J.* **35**, 866–880

40. Mauthe, M., Orhon, I., Rocchi, C., Zhou, X., Luhr, M., Hijlkema, K. J., *et al*. (2018) Chloroquine inhibits autophagic flux by decreasing autophagosome-lysosome fusion. *Autophagy* **14**, 1435–1455
41. Buratta, S., Tancini, B., Sagini, K., Delo, F., Chiaradia, E., Urbanelli, L., *et al*. (2020) Lysosomal exocytosis, exosome release and secretory autophagy: the autophagic- and endo-lysosomal systems go extracellular. *Int. J. Mol. Sci.* **21**, 2576
42. Gonzalez, C. D., Resnik, R., and Vaccaro, M. I. (2020) Secretory autophagy and its relevance in metabolic and degenerative disease. *Front. Endocrinol. (Lausanne)* **11**, 266
43. Ejlerskov, P., Rasmussen, I., Nielsen, T. T., Bergstrom, A. L., Tohyama, Y., Jensen, P. H., *et al*. (2013) Tubulin polymerization-promoting protein (TPPP/p25alpha) promotes unconventional secretion of alpha-synuclein through exophagy by impairing autophagosome-lysosome fusion. *J. Biol. Chem.* **288**, 17313–17335
44. Zhang, M., Kenny, S. J., Ge, L., Xu, K., and Schekman, R. (2015) Translocation of interleukin-1beta into a vesicle intermediate in autophagy-mediated secretion. *Elife* **4**. https://doi.org/10.7554/eLife.11205
45. Kimura, T., Jia, J., Kumar, S., Choi, S. W., Gu, Y., Mudd, M., *et al*. (2017) Dedicated SNAREs and specialized TRIM cargo receptors mediate secretory autophagy. *EMBO J.* **36**, 42–60
46. Chandramouli, K., and Qian, P. Y. (2009) Proteomics: challenges, techniques and possibilities to overcome biological sample complexity. *Hum. Genomics Proteomics* **2009**, 239204
47. Mizushima, N., and Levine, B. (2010) Autophagy in mammalian development and differentiation. *Nat. Cell Biol.* **12**, 823–830